Outage Probability Analysis of Full-Duplex Amplify-and-Forward MIMO Relay Systems

by

Geeta Sankar Kalyan Jonnalagadda

A Thesis Presented in Partial Fulfillment
of the Requirements for the Degree
Master of Science

Approved July 2018 by the
Graduate Supervisory Committee:

Cihan Tepedelenlioğlu, Chair
Daniel Bliss
Oliver Kosut

ARIZONA STATE UNIVERSITY

August 2018

ABSTRACT

Multiple-input multiple-output systems have gained focus in the last decade due to the benefits they provide in enhancing the quality of communications. On the other hand, full-duplex communication has attracted remarkable attention due to its ability to improve the spectral efficiency compared to the existing half-duplex systems. Using full-duplex communications on MIMO co-operative networks can provide us solutions that can completely outperform existing systems with simultaneous transmission and reception at high data rates.

This thesis considers a full-duplex MIMO relay which amplifies and forwards the received signals, between a source and a destination that do not a have line of sight. Full-duplex mode raises the problem of self-interference. Though all the links in the system undergo frequency flat fading, the end-to-end effective channel is frequency selective. This is due to the imperfect cancellation of the self-interference at the relay and this residual self-interference acts as intersymbol interference at the destination which is treated by equalization. This also leads to complications in form of recursive equations to determine the input-output relationship of the system. This also leads to complications in the form of recursive equations to determine the input-output relationship of the system. To overcome this, a signal flow graph approach using Mason's gain formula is proposed, where the effective channel is analyzed with keen notice to every loop and path the signal traverses. This gives a clear understanding and awareness about the orders of the polynomials involved in the transfer function, from which desired conclusions can be drawn. But the complexity of Mason's gain formula increases with the number of antennas at relay which can be overcome by the proposed linear algebraic method. Input-output relationship derived using simple concepts of linear algebra can be generalized to any number of antennas and the computation complexity is comparatively very low.

For a full-duplex amplify-and-forward MIMO relay system, assuming equalization at the destination, new mechanisms have been implemented at the relay that can compensate the effect of residual self-interference namely equal-gain transmission and antenna selection. Though equal-gain transmission does not perform better than the maximal ratio transmission, a trade-off can be made between performance and implementation complexity. Using the proposed antenna selection strategy, one pair of transmit-receive antennas at the relay is selected based on four selection criteria discussed. Outage probability analysis is performed for all the strategies presented and detailed comparison has been established. Considering minimum mean-squared error decision feedback equalizer at the destination, a bound on the outage probability has been obtained for the antenna selection case and is used for comparisons. A cross-over point is observed while comparing the outage probabilities of equal-gain transmission and antenna selection techniques, as the signal-to-noise ratio increases and from that point antenna selection outperforms equal-gain transmission and this is explained by the fact of reduced residual self-interference in antenna selection method.

ACKNOWLEDGMENTS

Firstly, I would like to thank my advisor Dr. Cihan Tepedelenlioğlu, for his continuous support and supervision. His guidance and encouragement played a vital role and steered me in the right direction.

I would like to extend my sincere gratitude to my committee members, Professors Daniel Bliss and Oliver Kosut. Also, I would like to take this chance to thank all the faculty members, from whom I have learned so many things, including but not limited to Professors Andreas Spanias, Antonia Papandreou-Suppappola, Lina Karam, Sule Ozev, Fengbo Ren, Ahmed Alkhateeb.

I am grateful to my colleagues Xiaofeng Li, Abhilash, Ruochen Zeng, Ahmed Ewaisha for their support and patience for having fruitful discussions with me and answering my questions. Thanks to my friends Revanth, Harsha, Navya, Prajwal, Nanda Kishore, Mayank, Karthik, and many others who have supported and encouraged me during the tough times.

Finally, I wish to express my indebtedness to my parents Surya Bhagavan J, Ahalya Kumari J, family, and my best friend Vijayalakshmi, who always stand by me and encourage through thick and thin.

TABLE OF CONTENTS

CHAPTER Page

CHAPTER Page

LIST OF FIGURES

CHAPTER Page

Chapter 1

INTRODUCTION

1.1 WIRELESS CHANNEL CHARACTERISTICS

Wireless systems have brought a lot of advantages to our daily life when compared to the wired systems in terms of mobility, portability and installation complexity. But all these came at the cost of reduced data rates, low system bandwidth, high interference, and low reliability when compared to the same wired systems. Among all the elements of a wireless system, the element that makes it unique with a lot of pros and cons is the wireless channel. A wireless channel is an uncertain and complicated medium of communication, unlike the cable medium in wired systems. It is evident that, as a signal propagates through a wireless channel, it experiences a lot of random variations like fading, scattering, shadowing due to reasons like the distance of propagation, the obstructions in the path of propagation, the mobility of the objects. This forces the channel characteristics to vary randomly with time and thus making the received signal to be unreliable. To analyze the performance of the wireless systems, a thorough understanding of the wireless channels and their behavior in different regimes is very much necessary.

In wireless communications, as the signal propagates in a wireless channel over a certain distance from the transmitter to the receiver, the signal will experience attenuation, termed as fading, which is a random process and can be due to multiple reasons. Fading can be classified as large-scale and small-scale fading depending on the factor that induces it. Large-scale fading is induced by the factors like shadowing, transmission distance. Shadowing can be understood as the obstruction of the trans-

mitted signal by the presence of buildings, walls, mountains. In general, shadowing is high in urban areas than the rural areas for obvious reasons. This large-scale fading is practically impossible to eliminate but can be characterized using various path-loss models for analysis as discussed in [1]. We will look into small-scale fading in detail in the following sections.

1.1.1 Small-scale Fading Models

The variations in the signal strength due to the constructive and destructive interference of multi-path components, over the distances that are in the order of carrier wavelength are referred by small-scale fading. Multi-path components are the components of the same transmitted signal that are propagating through different channels with different delays from the transmitter to the receiver. This small-scale fading can be characterized by the various models among which a few are mentioned below [1].

Rayleigh Fading

Rayleigh fading is a statistical model that considers the variations in the signal strength randomly as per Rayleigh distribution. Without loss of generality, in a practical scenario, we can assume the presence of sufficiently many scatterers, and accordingly, multiple independent scattered components of the transmitted signal are received by the receiver. Based on this assumption, we can definitively say that the channel impulse response can be modeled as a Gaussian process with the help of the central limit theorem. Also, in the absence of a dominant multi-path component, the in-phase and quadrature components can be modeled as uncorrelated zero-mean complex values. Thus, the envelope of the received signal that has a Rayleigh distribution can be written as:

$$p_Z(z) = \frac{2z}{P_r} e^{-\frac{z^2}{P_r}} = \frac{z}{\sigma^2} e^{-\frac{z^2}{2\sigma^2}} \tag{1.1}$$

where, $\overline{P}_r = 2\sigma^2$ is the average received signal power and σ^2 is the variance of the in-phase and quadratic components of the received signal.

Ricean Fading

Ricean fading model is considered in scenarios where a dominant multi-path component is present when the transmitted signal experience scattering from sufficiently many scatterers in the propagation environment. In cases, the dominant multi-path component can be the line of sight (LOS) component. The envelope of the channel response with Ricean distribution is given by:

$$p_Z(z) = \frac{2z(K+1)}{\overline{P}_r} \exp\left(-K - \frac{(K+1)z^2}{\overline{P}_r}\right) I_0\left(2z\sqrt{\frac{K(K+1)}{\overline{P}_r}}\right), z \geq 0 \qquad (1.2)$$

where K is the Ricean Factor which is the ratio of the power in LOS component to the power in other multi-path components, $\overline{P}_r$ is the average received signal power and $I_0(.)$ is the zeroth order Bessel function of the first kind. For a Ricean factor $K = 0$, Ricean fading model exactly resembles the Rayleigh fading, i.e., there is no dominant multi-path component (LOS). And a Ricean factor $K = \infty$ indicates that there is no multi-path propagation and all it has the LOS component only. From the two facts mentioned, we can make a point that the Ricean factor K indicates the severity of the fading, a large K implying a very mild fading.

Nakagami-m Fading

Theoretically, depending on the presence or the absence of the LOS component, Ricean and Rayleigh fading models may seem to work perfectly. But practically, these models do not fit some experimental data which led to the evolution of a new and more general fading model, which can fit a wide variety of empirical measurements accordingly. This distribution is named Nakagami-m distribution [2] and its

probability density function is given as:

$$p_Z(z) = \frac{2m^m z^{2m-1}}{\Gamma(m)\overline{P}_r^m} \exp\left(-\frac{mz^2}{\overline{P}_r}\right), m \geq 0.5 \tag{1.3}$$

where, $m = \frac{\overline{P}_r^2}{\mathrm{E}\left[\left(z^2-\overline{P}_r\right)^2\right]}$ is defined as the ratio of moments called the fading figure, $\overline{P}_r$ is the average received signal power and $\Gamma(.)$ is the Gamma function. When $m = 1$, Nakagami-m resembles Rayleigh fading and for other values of m, an approximation of Ricean can be derived. Similar to the Ricean factor K, m also indicates the severity of the fading and $m = \infty$ corresponds to the non-fading channels.

1.2 MULTIPLE INPUT MULTIPLE OUTPUT (MIMO) SYSTEMS

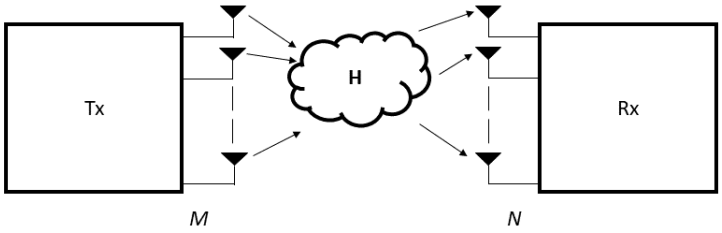

Figure 1.1: MIMO system - Transmitter with M antennas and Receiver with N antennas

MIMO systems refer to any system in which multiple antennas are used at both sides of the communication path as shown in Fig. 1.1. Although these systems create challenges in digital signal processing algorithms, which make them more complex when compared to single antenna systems, they provide greatly enhanced range and capacity. These clearly constructively examine the multi-path propagation by using multiple channels to the receiver. The traditional systems with a single antenna at both sides of the communication path are termed as single-input-single-output (SISO) systems, while systems with one transmit antenna and multiple receive antennas in a communication are termed as single-input-multiple-output (SIMO) systems and

the systems with multiple transmit antennas and one receive antenna in a communication are termed as multiple-input-single-output (MISO) systems. These different configurations in wireless communications are shown in the Fig. 1.2.

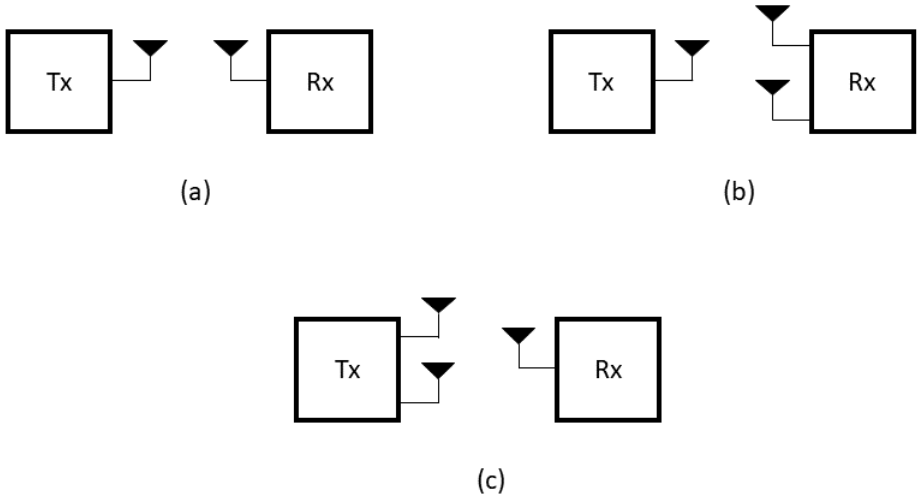

Figure 1.2: Different Space-Time systems: (a) SISO (b) SIMO (c) MISO

Considering M antennas at the transmitter and N antennas at the receiver as shown in the Fig. 1.1, let $\mathbf{x} = \begin{bmatrix} x_1 & x_2 & \cdots & x_M \end{bmatrix}^T$ be the transmitted signal, x_i being the signal transmitted on the i^{th} transmit antenna, $i \in \{1, 2, ..., M\}$. The received signal $\mathbf{y} = \begin{bmatrix} y_1 & y_2 & \cdots & y_N \end{bmatrix}^T$, y_j being the signal received on the j^{th} receive antenna, $j \in \{1, 2, ..., N\}$ is written as,

$$\mathbf{y} = \mathbf{H}\mathbf{x} + \mathbf{v} \tag{1.4}$$

where, $\mathbf{H}$ is an $N \times M$ channel matrix and $\mathbf{v}$ is an $N \times 1$ noise vector with zero mean and variance σ_ν^2.

1.3 CO-OPERATIVE NETWORKS

Co-operative networks in wireless communications are playing a very crucial role since last decade. Here, the required information is being shared by multiple radios

by interacting with each other in a wireless network. For a given transmission rate, achieving improved reliability or SNR of the information received, network coverage, and reduced power consumption has always been a motivation and led to the design of the cooperative networks [3]. To discuss further, let us consider the simplest scenario of cooperative networks, with a relay in between the source and destination nodes as shown in Fig. 1.3. A relay can simply be understood as a wireless transceiver that does some processing on the signal under transmission, so that the effects of the fading, path-loss can be compensated to a certain extent. The more generalized networks can have multiple sources, multiple destinations with multiple relays arranged in series or parallel, MIMO sources and MIMO destinations with MIMO relays in between [4–7]. We can find the heavy usage of these cooperative networks in urban areas where a signal can undergo heavy fading, and shadowing due to the presence of the buildings, so as to increase the efficiency of the communication. To discuss in detail

Figure 1.3: Relaying in cooperative networks with single relay between source and destination

about what actually happens at the relay, many different relaying strategies have been proposed during the past years that provided a substantial improvement in the overall performance and robustness. Among them, the most distinct and widely used strategies are amplify-and-forward or non-regenerative relaying strategy, decode-and-forward or regenerative relaying strategy.

1.3.1 Amplify-and-Forward (AF) Relaying

Relays operating with amplify-and-forward relaying strategy simply amplifies the received signal and retransmits it towards the next node ahead which can be either the destination or another relay connected in series or parallel. This process does not involve any coding or modulation methods i.e., it performs amplification of the signal only and hence it is called non-regenerative relaying [8, 9]. As the relays in this strategy just amplify the received signal and transmit it with different gain without any processing, there is a definite chance of enhancing the noise which is not the desired outcome of any technique [10]. However, for the same reason of no significant processing, the amplify-and-forward strategy has very low processing delay and very less computational or implementation complexity and this technique has been considered extensively in the context of various communication scenarios [3, 11, 12].

1.3.2 Decode-and-Forward (DF) Relaying

Relays that implement decode-and-forward relaying strategy decodes the received signal, re-modulates it with some encoding technique and retransmit to the next node ahead and hence is also called regenerative relaying [13, 14]. The complexity of decode-and-forward relaying when compared to amplify-and-forward relaying strategy is very much higher due to its full processing capabilities. It also requires a sophisticated media access control layer which is not even necessary in amplify-and-forward strategy. It is almost as complicated as a base station [15]. Now considering the performance of the strategies discussed, AF strategy has better performance than the DF strategy for uncoded BPSK modulation in terms of outage probability and

bit error rate [16]. Whereas for coded systems, DF strategy is proved to have better performance in terms of ergodic capacity, outage probability [17–19]

1.4 FULL-DUPLEX RELAYING

Duplex communication systems are those where devices can communicate with one another in both directions. These can be further classified into half-duplex and full-duplex systems based on how the two nodes transmit and receive [20, 21]. Applying this concept of duplex systems to co-operative networks, relaying techniques are discussed below.

1.4.1 Half-Duplex Relaying

Consider a source node and a destination node connected by a relay as shown in Fig. 1.3. Now, if the relay operates in half-duplex (HD) mode, then the relay can only receive the signal from the source or transmit its signal to the destination at a time. It cannot transmit and receive at the same time and thus, by using Time-Division Duplexing (TDD) [22], short time intervals will be allocated to the relay for transmitting and receiving the signal. The same principle can be extended to generalizations like multiple relays or a single MIMO relay.

1.4.2 Full-Duplex Relaying

If the relay operates in the full-duplex (FD) mode in the system shown in Fig. 1.3, then the relay can receive the signal from the source and transmit its signal to destination simultaneously. This full-duplex mode can be implemented using two different techniques namely, out-of-band full-duplex relaying and in-band full-duplex relaying. Out-of-band full-duplex relaying is same as frequency-division duplexing (FDD), where the transmission and reception at relay take place in different frequencies at

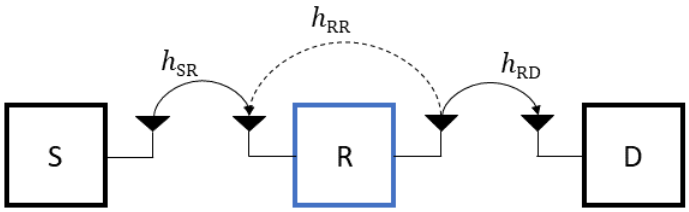

Figure 1.4: Full-Duplex Relaying in cooperative networks with single relay between source and destination

the same time [22], whereas on the contrary, in-band full-duplex (IBFD) relaying use same spectrum for both transmission and reception at the same time [23–25]. Transmission and reception in half-duplex relaying are done in same frequency band but at different time slots [26], resulting in complete elimination of interference between the incoming and outgoing signals at the relay. But this happens at the cost of doubling the total transmission time. Thus, we can definitively say that IBFD relaying is much more efficient than the half-duplex relaying in terms of system capacity, and the spectral efficiency is potentially doubled [21, 27].

Though out-of-band full-duplex relaying saves the transmission time, they still transmit and receive in different frequency bands and hence, they are not as efficient as IBFD relaying. This can be extended to systems with multiple relays arranged in series or parallel between source and destination which can either have single or multiple antennas at all the nodes [28–34]. Hereafter, FD systems considered in this thesis are referred to IBFD systems. The major problem in these systems is the self-interference (SI) at the relay, that is caused by transmitting and receiving at the same time in the same spectrum which can be seen in the Fig. 1.4. This SI can be mitigated by few cancellation techniques which are discussed in chapter 2, but

there will be a residual self-interference (RSI) left even after the cancellation and this constrains the performance of the system.

1.5 PREVIOUS WORKS IN FD MIMO CO-OPERATIVE NETWORKS

In this section, we will see various research works that are being done from a long time on full-duplex co-operative relay networks to discuss the problems involved, solutions found by various researchers and to determine the leftover open problems. In 5G, the applicability of full-duplex radios is explored, including those that address the challenges like flexible spectrum allocations and spectral efficiency with simultaneous enhancement in system throughput [25, 35–38].

In [39], the author discussed outage performance of a two-hop cooperative full-duplex relay with the amplify-and-forward scheme and detailed analysis with and without RSI has been provided and a lower bound for outage probability is presented. As an extension, in [40], the author has provided end-to-end input-output relationship using signal-flow graph approach for multi-hop full-duplex amplify-and-forward relaying with a multiple number of relays between the source and destination. The outage performance was analyzed with a matched filter and different equalizers and are compared with the half-duplex systems. In [41], an equal gain transmission technique (EGT) was designed for MIMO systems and a conclusion was made from the results that, irrespective of the increase in the number of transmit antennas, the SNR loss of a well-designed equal-gain transmission (EGT) system is at most 1.05 dB both in MISO and MIMO channels. Also, the comparison of EGT with optimal maximal ratio transmission (MRT) has been discussed and intuitively, we can say that MRT requires information about both phase and magnitude of channels, whereas EGT requires only the phase information, which gives EGT, the implementational advantages over MRT at the cost of compromised performance. In [42], transmit

beam-forming techniques with antenna selection and power combining in MIMO systems with multiple separate power amplifiers have been introduced. This is purely on MIMO systems without any relays in between the source and destination. The SNR gain of the proposed antenna selection schemes is compared with the equal-gain transmission technique.

In [34, 43–46], the performances of transmit antenna selection with generalized selection combining and maximal ratio combining have been deeply studied and different results have been produced. In [47], authors have proposed two different antenna-selection strategies where one of them aims at maximizing the received SNR at destination by selecting the antenna pair with maximum channel gain in the source-destination and relay-destination channels. While the other targets the maximization of SNR in the source-relay and the relay-destination channels by selecting the antenna pair with maximum channel gain in the source-destination and relay-destination channels. In this work, the author considered line of sight links along with the relay links and the relay is operated as per decode-and-forward principle and all the nodes are considered to have multiple antennas. Different power allocation schemes, optimal training for RSI, different channel estimation techniques for one-way and two-way relay networks have been proposed and discussed [48–52].

1.6 CONTRIBUTIONS AND OUTLINE OF THESIS

In wireless communications, spectral efficiency has become the prime objective and all the research works are directed towards this. One such potentially capable technique is full-duplex communication, as it can double the spectral efficiency when compared to the traditional half-duplex systems. Different models in full-duplex systems like the ones with multi-hop networks or multi-antenna networks add new capabilities to the co-operative networks by achieving higher data rates and enhanc-

ing the reliability along with simultaneous transmission and reception. However, as discussed in the earlier sections, full-duplex systems are not widely used due to the RSI.

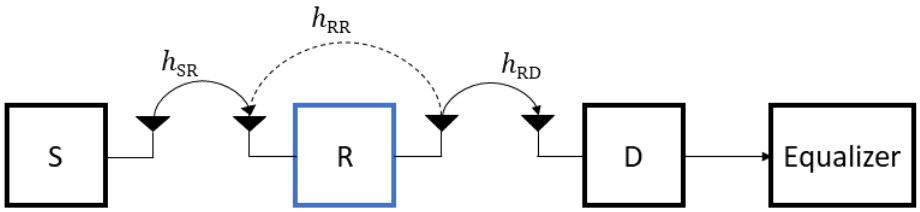

Figure 1.5: Full-Duplex Relaying in cooperative networks with equalizer at the destination

As mentioned earlier in the previous section, FD relays pose limitations due to RSI, which if addressed and resolved, can double the spectral efficiency. It can be clearly seen and understood from Fig. 1.5, that there raises an interference at the relay, due to simultaneous transmission and reception in the same frequency, which can be seen as a feedback loop at and persists even after implementing some cancellation techniques. Due to this RSI, even all the individual links in the system are assumed to undergo frequency flat fading, the end-to-end effective channel will be frequency selective. At the destination, this RSI acts as intersymbol interference (ISI) and can be canceled mostly by deploying an equalizer which can be of many types discussed in chapter 4.

The input-output relationship of the end-to-end system with a MIMO relay is derived with efficient approaches which can be generalized to any system. The relay is considered to be MIMO so that many digital signal processing aspects that can help in better SI reduction can be exploited. Transmit combining techniques namely equal-gain transmission (EGT) and antenna selection (AS) with different selection criteria are implemented at the relay. The equalizers at the destination are considered to

be of infinite length, which have a closed form expression for the output signal to noise ratio (SNR). Using such expressions, and considering the outage probability as a metric for performance analysis, different proposed strategies are computed and compared.

The organization of this thesis is done as described. In Chapter 2, the basic concepts that are required to understand the benefits of MIMO and full-duplex communications are discussed in detail. It also gives a comprehensive understanding of the residual self-interference (RSI) in full-duplex systems and different techniques to mitigate RSI. In Chapter 3, the input-output relationship of the system considered is derived by using the signal-flow graph approach with Mason's gain formula. The difficulties with increasing the number of antennas in using Mason's gain formula are discussed and as a solution, we derived expressions with the help of pure linear algebra. Chapter 4 provides the outage probability analysis for the proposed strategies that are to be implemented at the relay with equalization at the destination. The end-to-end SNR of the system is computed with different equalizers and the outage performances of proposed techniques are analyzed. Finally, Chapter 5 presents the conclusion of this thesis and the scope for future research in the area of full-duplex co-operative networks.

1.7 SUMMARY

In this chapter, we discussed the basic wireless channel characteristics and the fading models that benefit us in analyzing different systems. Subsequently, we established a basic understanding of MIMO systems and discussed different trends in co-operative networks. A detailed discussion of different relaying strategies amplify-and-forward, decode-and-forward has been presented. Full-duplex relaying and its advantages over half-duplex relaying are discussed, along with the problems it can

cause in the form of self-interference are explored. Different research ideas and previous works on the interference suppression in full-duplex systems are discussed and finally, the contributions and outline of this thesis are presented.

Chapter 2

REVIEW OF MULTI-ANTENNA SYSTEMS AND SI MITIGATION IN FD SYSTEMS

In this chapter, we will discuss the basic background knowledge that is required to understand the MIMO systems and the diversity techniques, along with detailed discussion about the SI cancellation techniques in FD systems.

2.1 BENEFITS OF MULTI-ANTENNA SYSTEMS

The multi-antenna systems significantly enhance the range and capacity compared to single antenna systems. Going into details, the benefits that are broadly viewed and analyzed are discussed in this section. Few very important advantages of the multi-antenna systems are array gain, diversity gain, multiplexing gain, and interference reduction [53].

2.1.1 Array Gain

The average increase in the received signal power is known as Array gain and is always proportional to the number of receiving antennas. It is rather easy to compute and understand in SIMO systems, where, with the knowledge of channel at the receiver, all the components on different receive antennas can be coherently combined, resulting in an improved overall SNR. The same can be implemented at the transmitter in MISO systems using beam-forming, but only with the complete channel knowledge. The array gain in the MIMO systems depends on the number of transmit and receive antennas.

2.1.2 Interference Reduction

In the wireless communications, interference is mainly due to the fact of frequency reuse. To be specific, the interference we are discussing here is about the inter-channel interference (ICI), which is a very frequent problem in wireless mobile networks. This ICI adds up to the overall noise and diminishes the SNR of the final output. Using multiple antennas, the receiver can exploit the fact of different spatial features of the desired signal and the ICI and thereby increase the overall SNR of the output. Again, the same gain can be obtained from the transmitter by using beam-forming and avoiding the ICI.

2.1.3 Diversity Gain

Diversity in wireless channels is for the sole purpose of fighting fading. Using multiple antennas, we create multiple paths of propagation for the transmitted signal, and thus the fading on all these links will be made statistically independent. Due to the diversity, we can assure that no two multi-path components undergo deep fade at the same time instant and the receiver can access all these components. Thus, we can observe an increase in the reliability of the received signal. As the number of paths for propagation increase, the diversity will increase and thus, lead to an enhanced SNR at the receiver. The diversity gain in SIMO and MISO systems can be defined as the number of receiving and transmitting antennas respectively. Whereas in MIMO systems, the diversity gain is equal to the number of independent channels of the system. Different techniques to achieve diversity are discussed in detail in the later sections.

2.1.4 Multiplexing Gain

This is one such benefit that can differentiate MIMO from other systems. This can be obtained only with multiple antennas on both sides of the communication path. This is achieved by spatial multiplexing, where the symbol stream to be transmitted is divided into multiple sub-streams, modulated and transmitted from separate antennas as shown in Fig. 2.1. Assuming ideal channel conditions, where the spatial features

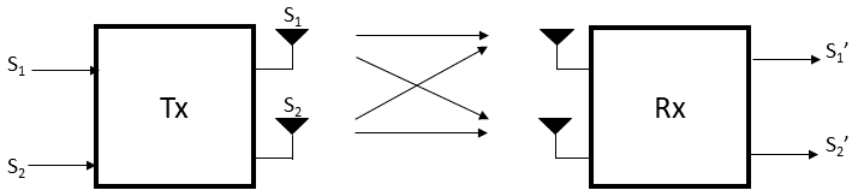

Figure 2.1: Multiplexing Gain in MIMO Systems, where Tx transmits 2 different signal streams S_1, S_2 instead of a single stream and each antenna at Rx receives copies of the 2 signals.

of the sub-streams transmitted are well separated, ideally orthogonal, the receiver can decode the sub-streams perfectly and thus increase the capacity of the channel or the throughput of the system. This increase in the channel capacity is termed as Multiplexing Gain.

2.2 DIVERSITY TECHNIQUES

As mentioned earlier, diversity is a technique used to overcome the effects of the channel fading, whose basic principle is to obtain multiple copies of a transmitted signal over multiple statistically independent channels of different strengths, such that at least one or more copies received will not be in a fade at a given instant of time, and thus making it possible to attain adequate signal power at the receiver. We

can intuitively say that, in the absence of diversity, to attain adequate power on the received signal, the transmitter needs to transmit at higher power levels in order to overcome fading, which is not convenient in most of the systems [54]. The diversity techniques can be broadly classified as Microdiversity, which can mitigate the effects of multipath fading and Macrodiversity, that mitigate the effects of shadowing. In this thesis and also in general, Microdiversity techniques are the ones under study. The most commonly used microdiversity techniques are discussed in detail below [1, 55, 56]:

2.2.1 Time Diversity

In this diversity technique, multiple versions of the same signal are transmitted at different time instants, that have a minimum separation of coherence time of the channel. This can be implemented by spreading the signal across the time by interleaving and transmitting the signal, thus obtaining the statistically independent fading. Due to the interleaving at the transmitter, the decoder at receiver experiences delays, making this technique very much effective in fast fading channel environments where the coherence time is small. Whereas, for the channels with large coherence times, i.e., slow fading channels, large inter-leavers are required which is not practically applicable in delay sensitive applications such as voice transmission. Also, it can be clearly seen that it does not have efficient spectral utilization due to the redundancy caused by interleaving in the time domain.

2.2.2 Frequency Diversity

Here, the same signal is transmitted at different frequencies that are separated by more than the coherence bandwidth of the channel, making the fading on each

channel to be statistically independent and thus, making sure that no two signals on different frequencies have a deep fade at the same time.

2.2.3 Spatial Diversity

This is one of the oldest and widely used techniques, where the transmitted signal is received on multiple antennas and these received components are further processed using different principles discussed in later sections. Irrespective of the processing method, the effectiveness of diversity is effected by the correlation of signals at different receiving antennas. This can be overcome by an adequate spacing between the antennas, such that minimum uncorrelated fading of antenna outputs is obtained. This is easy to implement and also does not require additional spectrum resources. The spatial diversity can be further classified as:

Receive Diversity

In this case, we use multiple antennas at the receiver and the multiple received signal components are processed using different combining techniques and hence minimizing the effects of the multi-path fading and enhancing the quality of the received signal. But this is achieved at the cost of increased complexity and implementation at the receiver.

Transmit Diversity

In this technique, we use multiple antennas at the transmitter instead of the receiver as in the previous case. The advantage of such transmit diversity is exploited by different signal processing techniques at the receiver. In general, this requires complete channel state information (CSI), at the transmitter. But with the help of space-time coding

techniques like Alamouti's scheme [57], the transmit diversity can be achieved without CSI.

2.2.4 Polarization Diversity

As the reflection and diffraction processes depend on polarization, we can say that the horizontally and vertically polarized multi-path components will have statistically independent fading on the signals. With the help of a dual-polarized antenna at the receiver, the differently polarized signals can be processed separately and thereby achieve diversity. The constraint on the minimum spacing between the antenna elements can be eliminated by this technique.

2.3 DIVERSITY COMBINING TECHNIQUES

In the previous section, we discussed how the signal received can be made reliable using the concepts of different diversity techniques. Using these basic diversity techniques, we can establish the channels for multi-path propagation that undergo statistically independent fading. But to achieve improved SNR levels at the receiver, the signals from various receiving antennas can be combined using different algorithms, which we are going to discuss in this section.

2.3.1 Selection Combining

Selection Combining (SC) is the simplest diversity technique and does not have any complexities of processing the received signals on different antennas at the receiver. In this technique, the branch with the highest signal-to-noise ratio (SNR) is chosen and the corresponding signal is considered to be the final output. The block diagram for the selection combining is shown in the Fig. 2.2. Though it is only one branch used at any point of time during the transmission, we need to focus on the SNR over

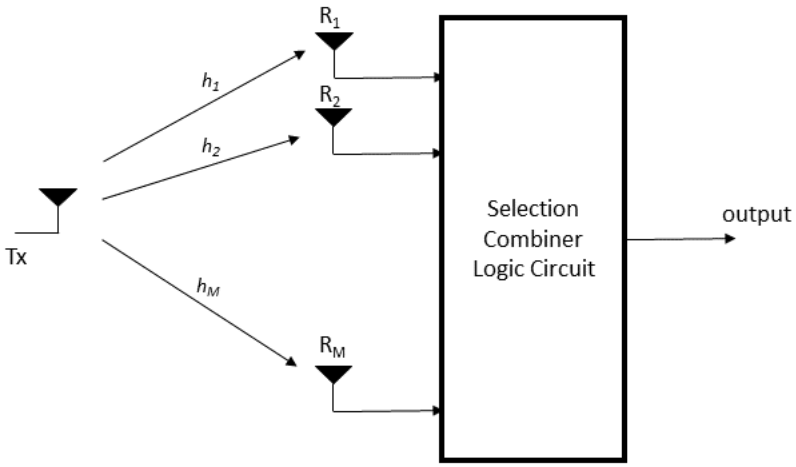

Figure 2.2: Block Diagram for Selection Combining

all the branches, as the branch with maximum SNR keeps varying depending on the coherence time of the channel. Considering γ_i to be the instantaneous SNR over the i^{th} branch, $i \in \{1, 2, ..., M\}$, the instantaneous SNR of the SC is given by:

$$\gamma_{\text{SC}} = \max\{\gamma_1, \gamma_2, ..., \gamma_M\} \tag{2.1}$$

and $\gamma_i = \frac{E_s}{N_0} |h_i|^2$, where E_s is the transmitted symbol energy and N_0 is the noise power spectral density.

2.3.2 Maximal Ratio Combining

In SC, we have seen that the branch with maximum SNR among all is set to be the output. Whereas, here in Maximal Ratio Combining (MRC), the branches are scaled with respect to their individual SNRs and all these branches are added to give the final output. This can be seen in the Fig. 2.3. The weights on the branches α_i are nothing but the complex conjugates of the channels h_i, where h_is are circularly symmetric complex Gaussian channel gains and thus, these weights need to have both

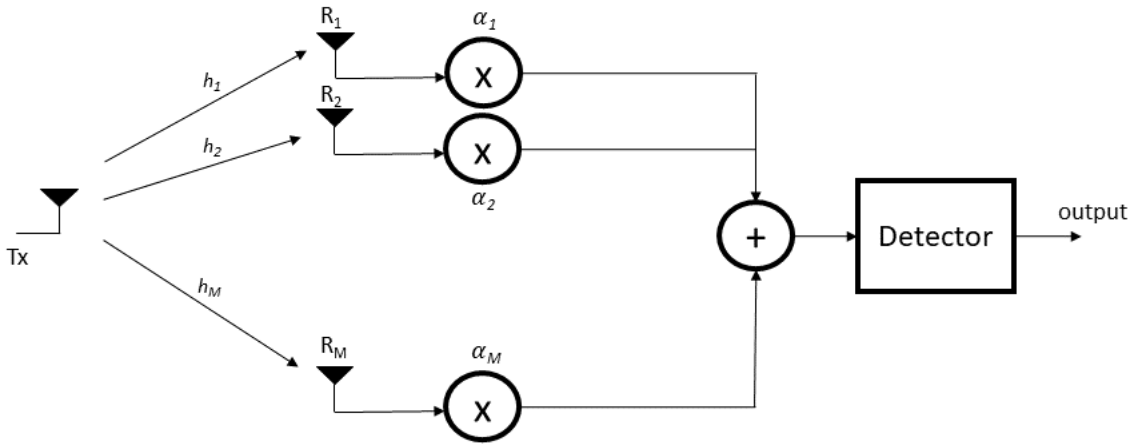

Figure 2.3: Block Diagram for Maximal Ratio Combining

the phase and magnitude information of the channels.

$$\alpha_i = h_i^* = |h_i| \, e^{-j\angle h_i} \tag{2.2}$$

From the weights of the branches, it is evident that, to implement maximal ratio combining, we need the knowledge of both the amplitude and phase of the channels. The received signal on each branch $y_i(t)$ is given by,

$$y_i(t) = \sqrt{\Gamma} h_i x(t) + \nu_i(t) \tag{2.3}$$

where $x(t)$ is the transmitted signal, Γ is the average SNR of the channel and ν_i is the noise component at the i^{th} receiving antenna. Now, after scaling these individual signals on all the branches with the corresponding weights α_i, the combiner output $y_{\mathrm{MRC}}(t)$ is given by,

$$y_{\mathrm{MRC}}(t) = \sum_{i=1}^{M} y_i(t)\alpha_i = \sqrt{\Gamma} \sum_{i=1}^{M} \alpha_i h_i x(t) + \sum_{i=1}^{M} \alpha_i \nu_i(t) \tag{2.4}$$

Assuming that the noise at all the branches are statistically independent, the average output SNR is given by,

$$\begin{aligned}\Gamma_{\mathrm{MRC}} &= \frac{\mathrm{E}\left[\left|\sqrt{\Gamma}x(t)\sum_{i=1}^{M}\alpha_i h_i\right|^2\right]}{\mathrm{E}\left[\left|\sum_{i=1}^{M}\alpha_i\nu_i(t)\right|^2\right]} \\ &= \frac{\Gamma E_s}{N_0}\frac{\mathrm{E}\left[\left|\sum_{i=1}^{M}\alpha_i h_i\right|^2\right]}{\mathrm{E}\left[\left|\sum_{i=1}^{M}\alpha_i\right|^2\right]}\end{aligned} \tag{2.5}$$

From above, the instantaneous SNR, γ_{MRC} of the MRC combiner can be given by,

$$\gamma_{\mathrm{MRC}} = \frac{\Gamma E_s}{N_0}\frac{\left|\sum_{i=1}^{M}\alpha_i h_i\right|^2}{\left|\sum_{i=1}^{M}\alpha_i\right|^2} \tag{2.6}$$

Now, using Cauchy-Schwartz inequality for complex numbers [58], we have

$$\left|\sum_{i=1}^{M}\alpha_i h_i\right|^2 \leq \sum_{i=1}^{M}|\alpha_i|^2\sum_{i=1}^{M}|h_i|^2 \tag{2.7}$$

and the equality holds as $\alpha_i = h_i^*$, and thus leading to,

$$\gamma_{\mathrm{MRC}} = \frac{\Gamma E_s}{N_0}\sum_{i=1}^{M}|h_i|^2 \tag{2.8}$$

From the above equation, it can be viewed that the maximal ratio combiner output SNR is the sum of instantaneous SNRs over all the branches. Thus, we can say that, MRC performs optimal combining.

2.3.3 Equal Gain Combining

Equal-Gain Combining (EGC) is almost similar to the maximal ratio combining, except for the difference that all the branches are scaled with equal weights unlike MRC, and these weights simply co-phase the channels, i.e., they only have phase

information of the channels. We can say that EGC is next to MRC in performance. Referring to Fig. 2.3, the weights on each branch α_is will now be given as:

$$\alpha_i = e^{-j\angle h_i} \tag{2.9}$$

The received signal at each antenna is same as in (2.3), and the EGC combiner output $y_{\text{EGC}}(t)$ is given by:

$$y_{\text{EGC}}(t) = \sum_{i=1}^{M} y_i(t) = \sqrt{\Gamma} \sum_{i=1}^{M} \alpha_i h_i x(t) + \sum_{i=1}^{M} \alpha_i \nu_i(t) \tag{2.10}$$

Following the same mathematical simplification as we did in MRC, the instantaneous SNR, γ_{EGC} of the EGC combiner is given by

$$\gamma_{\text{EGC}} = \frac{\Gamma E_s}{N_0 M} \sum_{i=1}^{M} |h_i|^2 \tag{2.11}$$

2.4 MITIGATION OF SI IN FD RELAYING

Recalling the discussion we presented in sections 1.4 and 1.5, with all the advantages IBFD provides, it also poses a major disadvantage which needs a powerful solution for these systems to be widely used in the industry. The disadvantage is that, during the course of transmission, the receiver side of the relay receives the signal transmitted by itself along with the signal transmitted by the source and this phenomenon is named as self-interference (SI) [59–63]. It is because of this setback, IBFD systems are not being deployed as widely as half-duplex systems [64]. This SI cannot be simply removed just because we have the knowledge of transmitted and received signals. Significant research has been going on for few years by the researchers and important interference cancellation techniques have been proposed which are the propagation-domain cancellation, the analog-domain cancellation, the digital-domain cancellation [23].

2.4.1 Propagation-Domain SI Cancellation

The interference cancellation in the propagation-domain is achieved by isolating the transmitter chain from the receiver chain. In case of shared-antenna systems, where the same antenna functions as transmitter and receiver, isolation can be obtained by using circulator, whereas, in separate antenna systems, the same isolation can be attained by a combination of path-loss, cross polarization, and antenna directionality [65–68]. Path-loss can be achieved by spacing the transmitter and receiver far enough or by placing absorptive shielding between them. Cross polarization is acquired just by making the transmit antenna to transmit horizontally polarized signals and the receive antenna to receive vertically polarized signals, so as to avoid interference. These are not much effective in suppressing the reflected path SI and also the major set back in this technique is that the desired signal also might accidentally get suppressed along with the undesired SI.

2.4.2 Analog-Domain SI Cancellation

The suppression of the self-interference in this analog-domain cancellation technique occurs before the analog-to-digital conversion. One of the methods to achieve the suppression is to tap the transmitted signal at the transmit antenna feed and is removed from the receive antenna feed after it is electronically processed in analog circuit domain. By tapping the outgoing signal as close as possible to the transmit antenna, this technique can observe the non-idealities of the system like oscillator phase noise and power amplifier distortion. With the knowledge of the channel, this technique can suppress both direct and reflected path interference [59, 63, 65, 69–72]. Although it provides significant advantages like knowledge about the non-idealities of the transmitter, it needs a lot of analog signal processing which can turn out to be

more complex than that is expected for wideband signals, especially while suppressing the reflected-path interference with the knowledge of channel. This analog signal processing has more complexity in hardware than the digital signal processing.

2.4.3 Digital-Domain SI Cancellation

In digital-domain cancellation technique, the interference is suppressed after the analog-to-digital conversion by using very sophisticated digital signal processing techniques on the received signal [23]. However, as the processing is done in the digital domain, the dynamic range of the analog-to-digital domain converter plays a major role and that limits the desired suppression. Therefore, to attain significant suppression of the self-interference, sufficient suppression must be attained before the signal is converted to the digital domain, i.e., in propagation and analog domain. Thus, by using all the techniques discussed, propagation-domain, analog-domain, digital-domain cancellations in a sequence, we can limit the effect of SI to a great extent.

2.5 SUMMARY

In this chapter, to summarize, the exclusive benefits of MIMO systems like array gain, diversity gain, interference reduction and multiplexing gain are discussed, followed by presenting in-depth details about the techniques that can be implemented to achieve diversity. In spatial diversity, different combining techniques like selection combining, maximal ratio combining, equal-gain combining are explored. Subsequently, few techniques that are being implemented widely and that can help in the self-interference cancellation in different phases of transmission are discussed and it is suggested to perform propagation-domain, analog-domain and digital-domain cancellation techniques in sequence to attain a significant level of cancellation.

Chapter 3

FULL-DUPLEX AMPLIFY-AND-FORWARD MIMO RELAYING

In this chapter, we start with introducing the system model that is under consideration and then we proceed with two different methods to derive the input-output relationship of the system explained in detail. Firstly, for easy understanding a simple full-duplex MIMO relay with 2 transmit and receive antenna pairs is considered for study and later, this is generalized to relay with M transmit and receive antenna pairs. From here on, in this thesis, interference is referred to RSI, which means the SI remained after three cancellation techniques discussed in chapter 2 are implemented in sequence.

3.1 SYSTEM MODEL

A full-duplex amplify-and-forward MIMO relaying system as shown in Fig. 3.1, consists of a source node, S, a destination node, D, with a single antenna at each of them. There is no direct link between them and are connected through a MIMO relay node, R, with M transmitting and M receiving antennas. The relay continuously amplifies and forwards the symbols received from S in previous time-slots while receiving new symbols, with a processing delay of one symbol. Let $\mathrm{T}_i, \mathrm{R}_i$ denote the i^{th} transmit and receive antennas respectively, where $i \in \{1, 2, \cdots, M\}$. Let $\Gamma_{\mathrm{SR}}, \Gamma_{\mathrm{RR}}, \Gamma_{\mathrm{RD}}$ denote the average SNRs across the channels between S-R, R-R, and R-D respectively. h_i, h_{M+i} denote the channel gains between S-R and R-D respectively. In general, let the signal transmitted by S be $x[n]$ and the signal received by D be $y[n]$. The i^{th} receiving antenna of R, i.e., R_i receives a signal $r_i[n]$, which is the combination of signal transmitted by S, the RSI signal components from all the

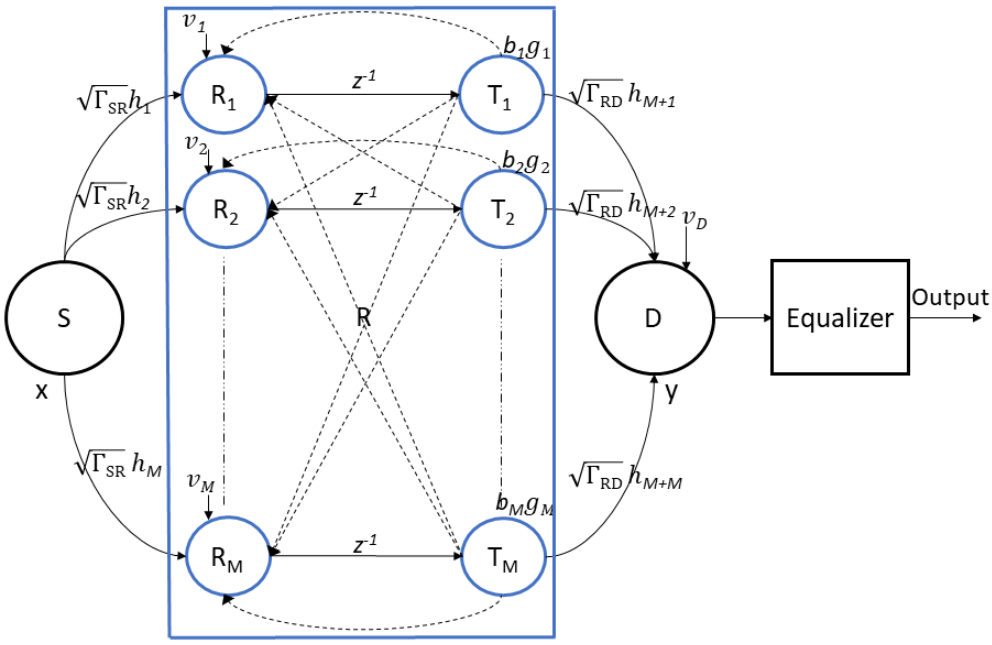

Figure 3.1: System model with source and destination nodes having one antenna without line of sight, connected by FD AF $M \times M$ Relay

transmitting antennas of R and the corresponding noise input signal, $\nu_i[n]$ at R_i:

$$\begin{aligned} r_i[n] &= \sqrt{\Gamma_{\mathrm{SR}}}h_i x[n] + \sqrt{\Gamma_{\mathrm{RR}}}h_{1i}t_1[n] + \sqrt{\Gamma_{\mathrm{RR}}}h_{2i}t_2[n] + \cdots + \sqrt{\Gamma_{\mathrm{RR}}}h_{Mi}t_M[n] + \nu_i[n] \\ &= \sqrt{\Gamma_{\mathrm{SR}}}h_i x[n] + \sum_{j=1}^{M}\sqrt{\Gamma_{\mathrm{RR}}}h_{ji}t_j[n] + \nu_i[n], \qquad i,j \in \{1,2,\cdots,M\} \end{aligned} \tag{3.1}$$

where h_{ji} is the channel from T_j to R_i and $t_j[n]$ is the signal transmitted by T_j. From hereon, the RSI channels of the system are represented by the dotted lines as shown in Fig. 3.1. In general, $t_i[n]$ is given by

$$t_i[n] = b_i g_i r_i[n-1] \tag{3.2}$$

where b_i is the pre-coding co-efficient, g_i is the amplification factor at T_i which will be discussed in detail in the consequent chapters. Once, after R amplifies and forwards the signal, the destination D receives the signal, $y[n]$, which is the combination of

signals from all T_is and the noise, $\nu_D[n]$ at D.

$$y[n] = \sqrt{\Gamma_{\mathrm{RD}}} \sum_{i=1}^{M} h_{M+i} t_i[n] + \nu_D[n] \tag{3.3}$$

We consider frequency-flat Rayleigh fading across the channels, so that $h_i, h_{M+i}, i \in \{1, 2, ...M\}$, are complex Gaussian channel gains with zero-mean and variance σ_h^2. The interference channels at R $h_{ij}, i, j \in \{1, 2, ...M\}$ are also considered to be frequency-flat Rayleigh fading with zero-mean and variance σ_r^2. We can clearly see that the RSI at R makes the effective channel of the system to be frequency-selective. We assume all the channels in the system to be independent and the additive Gaussian noise components, ν_D, at the destination and ν_i at R, have an identical variance, σ_ν^2. To make things simple and convenient for deriving input-output relationship, from here on, without loss of generality, we assume $\sigma_h^2 = \sigma_r^2 = \sigma_\nu^2 = 1$.

3.2 MASON'S GAIN FORMULA APPROACH TO FIND INPUT-OUTPUT RELATIONSHIP OF THE SYSTEM

From (3.1), (3.2), the input-output relationship can be established by recursive substitution process. As we transmit finitely large sequence signal from S, over a duration, this recursive method will turn to be complex and tedious. Hence, we propose the signal flow graph approach that reduces the complexity to a significant extent.

3.2.1 Signal Flow Graph

The signal flow graph is a graphical approach for solving a system of linear equations invented by Claude Elwood Shannon, an American mathematician, also known as "the father of information theory". In literature, we have two methods proposed [73, 74] that closely use the signal flow graph approach and they have been great

aids in achieving the in-depth knowledge about the structure and nature of solutions of systems of equations. But the approach by Mason [74] has been widely approved years after it was proposed and since then, signal flow graph is called Mason's graph. This is a directional graph in which there are multiple nodes with their respective variables that are involved in the system. The arrows represent the functional connection between the nodes with the multiplying factor above them and these are clearly explained in the section 3.2.3.

3.2.2 Mason's Gain Formula

To find the overall transfer function of a network with multiple nodes, where inputs and outputs are present at any node, Samuel J. Mason [74] proposed an efficient method which is named after him as Mason Gain Formula (MGF). Though there are techniques other than MGF, like the block reduction method, MGF yields the result with a simple and direct procedure without much complexity. It analyzes the signal flow graph to find the transfer function of the overall system. The terminology of different parameters required in the computation of MGF is explained in detail below:

- Path: A continuous set of branches traversed in the direction indicated by them.
- Forward Path: A path from the input node to the output node, without traversing a node more than once.
- Loop: A path starting and ending at the same node, without traversing a node more than once during its course.
- Path Gain: The product of gains on all the branches in the path.
- Loop Gain: The product of gains on all the branches in the loop.

- Non-touching Loops: Loops that do not traverse through any common node.

The Mason's Gain Formula is given by,

$$G = \frac{y(z)}{x(z)} = \frac{\sum_{k=1}^{W} G_k \Delta_k}{\Delta} \tag{3.4}$$

$\Delta = 1 - \sum L_i + \sum L_i L_j - \sum L_i L_j L_k + \cdots + (-1)^m \sum \cdots + \cdots$

where, Δ = Determinant of the signal flow graph

$y(z)$ = Z-transform of the signal from the output node

$x(z)$ = Z-transform of the signal to the input node

G = Transfer function

W = Number of forward paths between $x(z)$ and $y(z)$

G_k = Path gain of the k^{th} forward path between $x(z)$ and $y(z)$

L_i = Loop gain of any loop in the system

$L_i L_j$ = Product of the loop gains of two non-touching loops

$L_i L_j L_k$ = Product of the loop gains of three non-touching loops

Δ_k = The co-factor value of Δ for k^{th} forward path, with the loops touching that path removed.

3.2.3 Mason Gain Formula analysis for 2×2 Full-Duplex Amplify-and-Forward MIMO Relay system

To explain the MGF in detail, consider a 2×2 full-duplex amplify-and-forward MIMO relay between the source and destination nodes as shown in the Fig. 3.2, whose corresponding signal-flow graph is given in Fig. 3.3. We can see from the signal-flow graph that, there are four forward paths $\mathrm{SR_1T_1D}$, $\mathrm{SR_2T_2D}$, $\mathrm{SR_1T_1R_2T_2D}$, $\mathrm{SR_2T_2R_1T_1D}$ with path gains $G_1 = \sqrt{\Gamma_{\mathrm{SR}}\Gamma_{\mathrm{RD}}} h_1 h_3 b_1 g_1 z^{-1}$, $G_2 = \sqrt{\Gamma_{\mathrm{SR}}\Gamma_{\mathrm{RD}}} h_2 h_4 b_2 g_2 z^{-1}$, $G_3 = \sqrt{\Gamma_{\mathrm{SR}}\Gamma_{\mathrm{RR}}\Gamma_{\mathrm{RD}}} h_1 h_{12} h_4 b_1 g_1 b_2 g_2 z^{-2}$, and $G_4 = \sqrt{\Gamma_{\mathrm{SR}}\Gamma_{\mathrm{RR}}\Gamma_{\mathrm{RD}}} h_2 h_{21} h_3 b_1 g_1 b_2 g_2 z^{-2}$ respectively. The individual loops are $\mathrm{R_1T_1R_1}$,

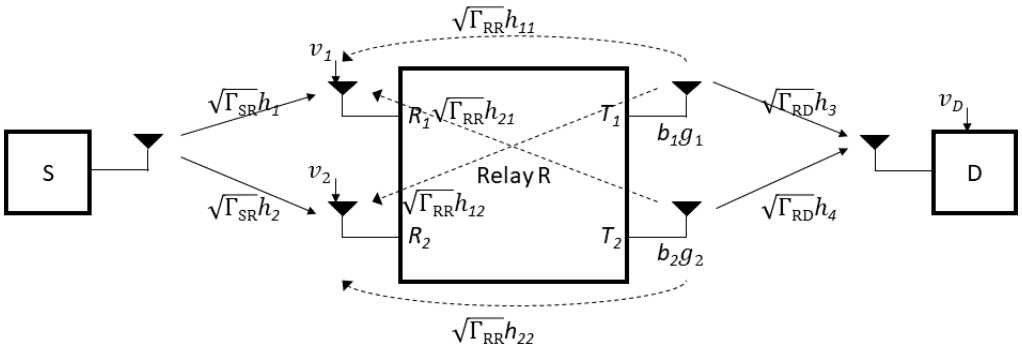

Figure 3.2: Block Diagram for a system with 2×2 FD AF Relay

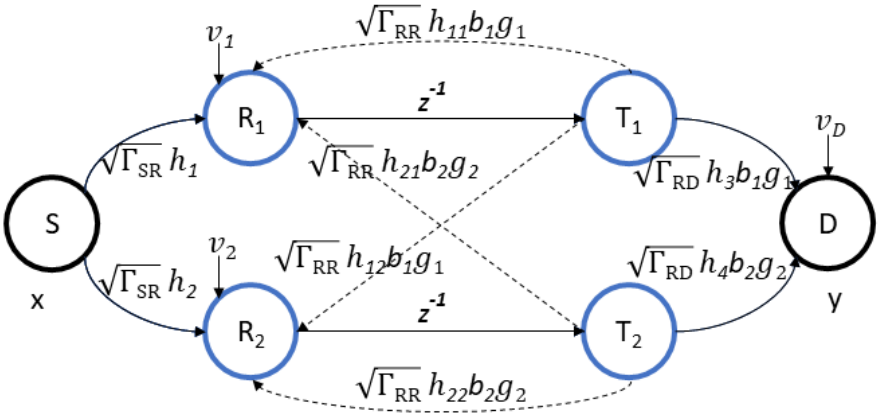

Figure 3.3: Signal-Flow Graph for a system with 2×2 FD AF Relay

$R_2T_2R_2$, $R_1T_1R_2T_2R_1$, with loop gains $L_1 = \sqrt{\Gamma_{RR}}h_{11}b_1g_1z^{-1}$, $L_2 = \sqrt{\Gamma_{RR}}h_{22}b_2g_2z^{-1}$, $L_3 = \Gamma_{RR}h_{12}h_{21}b_1g_1b_2g_2z^{-2}$. The product of two non-touching loops is L_1L_2 corresponding to the loops $R_1T_1R_1$, $R_2T_2R_2$.

It is evident from (3.4), that the transfer function represents the input-output relationship of the system. Since, we have two noise inputs, one information signal input, and one output, we write three input-output relationship equations with respect to each of the three inputs of the system. Since the output of the system is a linear function of the input and noise processes, we can apply linearity and find

the overall input-output relationship including noise. The overall transform-domain input-output relationship of the system can be written as,

$$y(z) = H_s(z)x(z) + H_{\nu_1}(z)\nu_1(z) + H_{\nu_2}(z)\nu_2(z) + \nu_D(z) \tag{3.5}$$

We now proceed to find the effective channels $H_s(z), H_{\nu_1}(z), H_{\nu_2}(z)$, with respect to information and noise inputs at the relay R, respectively.

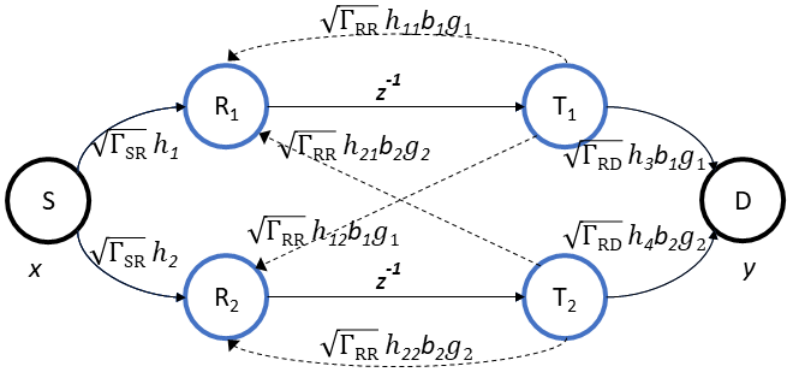

Figure 3.4: Signal-flow graph for a system with 2×2 FD AF Relay with respect to Symbol Input

- **Effective Channel for Signal from S:** While deriving this, we neglect the noise inputs ν_1, ν_2 by assuming that they are absent. Thus, the signal-flow graph is modified as shown in Fig. 3.4.

$$H_s(z) = \frac{A + B}{1 - \sqrt{\Gamma_{RR}}\,(h_{11}b_1g_1 + h_{22}b_2g_2)\,z^{-1} + \Gamma_{RR}b_1g_1b_2g_2\,(h_{11}h_{22} - h_{12}h_{21})\,z^{-2}} \tag{3.6}$$

where $A = \sqrt{\Gamma_{SR}\Gamma_{RD}}\,(h_1h_3b_1g_1 + h_2h_4b_2g_2)\,z^{-1}$

$B = \sqrt{\Gamma_{SR}\Gamma_{RR}\Gamma_{RD}}b_1g_1b_2g_2\,(h_1h_{12}h_4 + h_2h_{21}h_3 - h_1h_{22}h_3 - h_2h_{11}h_4)\,z^{-2}$

- **Effective Channel for Noise ν_1 at R_1:** In this case, we assume all other inputs except ν_1 are absent. The modified signal-flow graph is shown in Fig. 3.5.

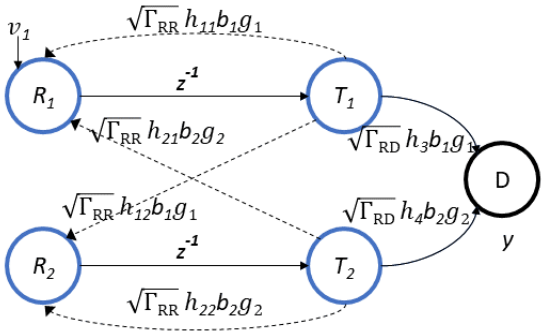

Figure 3.5: Signal-flow graph for a system with 2×2 FD AF Relay with respect to Noise Input at R_1

$$H_{\nu_1}(z) = \frac{\sqrt{\Gamma_{RD}}h_3b_1g_1z^{-1} - \sqrt{\Gamma_{RR}\Gamma_{RD}}b_1g_1b_2g_2\left(h_{22}h_3 - h_{12}h_4\right)z^{-2}}{1 - \sqrt{\Gamma_{RR}}\left(h_{11}b_1g_1 + h_{22}b_2g_2\right)z^{-1} + \Gamma_{RR}b_1g_1b_2g_2\left(h_{11}h_{22} - h_{12}h_{21}\right)z^{-2}} \tag{3.7}$$

- **Effective Channel for Noise ν_2 at R_2:** In this case, we assume all other inputs except ν_2 are absent. The modified signal-flow graph is shown in Fig. 3.6.

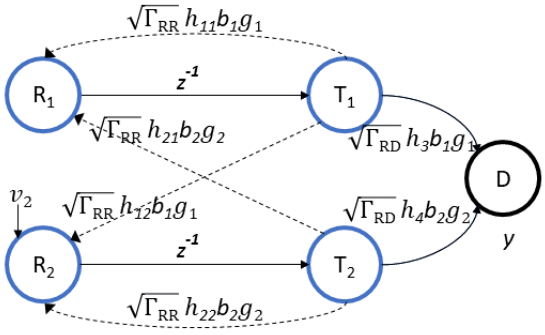

Figure 3.6: Signal-flow graph for a system with 2×2 FD AF Relay with respect to Noise Input at R_2

$$H_{\nu_2}(z) = \frac{\sqrt{\Gamma_{\mathrm{RD}}} h_4 b_2 g_2 z^{-1} - \sqrt{\Gamma_{\mathrm{RR}}\Gamma_{\mathrm{RD}}} b_1 g_1 b_2 g_2 \left(h_{11}h_4 - h_{21}h_3\right) z^{-2}}{1 - \sqrt{\Gamma_{\mathrm{RR}}}\left(h_{11}b_1 g_1 + h_{22}b_2 g_2\right) z^{-1} + \Gamma_{\mathrm{RR}} b_1 g_1 b_2 g_2 \left(h_{11}h_{22} - h_{12}h_{21}\right) z^{-2}} \tag{3.8}$$

3.2.4 Mason Gain Formula analysis for $M \times M$ Full-Duplex Amplify-and-Forward MIMO Relay system

Now, let us generalize our system by making the relay to have M number of transmit and receive antennas and then, we use Mason's gain formula to find the transfer functions with respect to all the inputs of the system. As we discussed earlier, the overall output of the system being a linear function of all the input and noise processes, the overall transform-domain input-output relationship of the system can be given as:

$$\begin{aligned} y(z) &= H_s(z)x(z) + H_{\nu_1}(z)\nu_1(z) + H_{\nu_2}(z)\nu_2(z) + \cdots + H_{\nu_M}(z)\nu_M(z) + \nu_D(z) \\ &= H_s(z)x(z) + \sum_{i=1}^{M} H_{\nu_i}(z)\nu_i(z) + \nu_D(z) \end{aligned} \tag{3.9}$$

As shown in Fig.3.1, we can see that, there are a total of $M+1$ inputs, that comprises of M noise inputs at M receive antennas of R and one symbol input from S. The transfer function for each of them is found by assuming that only one of them is present and all others are absent. The path gains and loop gains, in this case, will be much complex than what we have seen in a simple 2×2 MIMO relay system. Here, we provide with the generalized closed-form expressions for the gains of given paths and loops, from which the overall transfer function for any input component can be found.

- Forward Path: A forward path in this $M \times M$ Relay system can either include one transmit-receive antenna pair or multiple transmit-receive antenna pairs. Here, we provide with the path gains for both the cases.

For any k^{th} direct forward path that includes an i^{th} transmit-receive antenna pair only, the path gain can be found by:

$$G_k = \sqrt{\Gamma_{\mathrm{SR}}\Gamma_{\mathrm{RD}}} h_i h_{M+i} b_i g_i z^{-1}, \qquad i \in \{1, 2, ..., M\} \tag{3.10}$$

Whereas, for any k^{th} forward path that includes multiple antenna pairs, the path gain can be given by:

$$G_k = \sqrt{\Gamma_{\mathrm{SR}}\Gamma_{\mathrm{RD}}} h_{P_1} \left(\prod_{i=1}^{N-1} h_{P_i P_{i+1}} b_{P_i} g_{P_i} \right) h_{M+P_N} b_{P_N} g_{P_N} z^{-N} \tag{3.11}$$

where,

P is a set that can have a maximum of M values and the i^{th} element of P, $P_i \in \{1, 2, ..., M\}$ and N is number of elements in P ($N \leq M$).

- Loop: Similar to the forward path, a loop in an $M \times M$ Relay system can also either include one transmit-receive antenna pair or multiple transmit-receive antenna pairs. And we provide with the loop gains for both the cases.

  For a direct loop, i.e., a loop that includes an i^{th} transmit-receive antenna pair only, the loop gain can be found by:

$$L = \sqrt{\Gamma_{\mathrm{RR}}} h_{ii} b_i g_i z^{-1} \tag{3.12}$$

  If a loop includes multiple transmit-receive antenna pairs, the loop gain is given as:

$$L = \Gamma_{\mathrm{RR}}^{\frac{N}{2}} \left(\prod_{i=1}^{N-1} h_{P_i P_{i+1}} b_{Pi} g_{P_i} \right) h_{P_N P_1} b_{P_N} g_{P_N} z^{-N} \tag{3.13}$$

Using the expressions for the forward path and the loop, one can find the respective gains for any of the possible paths and loops and thus, by substituting thse in the MGF, we can obtain the transfer function of the system.

3.3 LINEAR ALGEBRA APPROACH TO FIND INPUT-OUTPUT RELATIONSHIP

The input-output relationship computed by MGF may seem less complex for small values of M, but as M increases, i.e., as the number of transmitting and receiving antennas at R increases, the number of forward paths and the loops increase massively and the computational complexity increases massively. Although there are benefits from using MGF, like the knowledge about the degree of the polynomials involved in the transfer function and number of paths that the signal can traverse can be known easily by looking at the expression, to reduce complexity we seek the help of linear algebra and make things simpler.

Let the M channels between source S and relay R, denoted as h_i in the previous sections be now combined and denoted in the vector form as $\mathbf{h}_{\mathrm{SR}}$ given by:

$$\mathbf{h}_{\mathrm{SR}} = \begin{bmatrix} h_1 & h_2 & \cdots & h_M \end{bmatrix}^{\mathsf{T}} \tag{3.14}$$

The M channels between relay R and destination D denoted as h_{M+i} earlier be now combined and denoted in the vector form as $\mathbf{h}_{\mathrm{RD}}$ given by:

$$\mathbf{h}_{\mathrm{RD}} = \begin{bmatrix} h_{M+1} & h_{M+2} & \cdots & h_{M+M} \end{bmatrix}^{\mathsf{T}} \tag{3.15}$$

The noise components at the M receiving antennas of the relay R denoted as ν_i be combined and denoted in the vector form as $\mathbf{v}$ given by:

$$\mathbf{v} = \begin{bmatrix} \nu_1 & \nu_2 & \nu_3 & \cdots & \nu_M \end{bmatrix}^{\mathsf{T}} \tag{3.16}$$

The RSI channels at the relay R denoted as h_{ji}, that represents the channel from T_j to R_i in the earlier sections be combined and denoted in the matrix form given by $\mathbf{H}$:

$$\mathbf{H} = \begin{bmatrix} h_{11} & h_{21} & \cdots & h_{M1} \\ h_{12} & h_{22} & \cdots & h_{M2} \\ \vdots & & \ddots & \\ h_{1M} & h_{2M} & \cdots & h_{MM} \end{bmatrix} \tag{3.17}$$

The amplification factors g_i at each T_i of the relay R be combined and given in the matrix form as $\mathbf{G}$ given by:

$$\mathbf{G} = \begin{bmatrix} g_1 & 0 & 0 & \cdots & 0 \\ 0 & g_2 & 0 & \cdots & 0 \\ \vdots & & & & \\ 0 & 0 & 0 & \cdots & g_M \end{bmatrix} \tag{3.18}$$

The pre-coding co-efficients b_i at each T_i of the relay R be combined and given in the matrix form as $\mathbf{B}$ given by:

$$\mathbf{B} = \begin{bmatrix} b_1 & 0 & 0 & \cdots & 0 \\ 0 & b_2 & 0 & \cdots & 0 \\ \vdots & & & & \\ 0 & 0 & 0 & \cdots & b_M \end{bmatrix} \tag{3.19}$$

The matrices $\mathbf{B}$ and $\mathbf{G}$ being diagonal matrices, we can exploit the symmetric property of the diagonal matrix, i.e., $\mathbf{B}^{\mathsf{T}} = \mathbf{B}$ and $\mathbf{G}^{\mathsf{T}} = \mathbf{G}$.

The signal received at each R_i given by $r_i[n]$ in (3.1) can now be combined and the signal received by M receiving antennas can be represented in the compact vector form as shown in equation below,

$$\mathbf{r}[n] = \sqrt{\Gamma_{\mathrm{SR}}}\mathbf{h}_{\mathrm{SR}}x[n] + \sqrt{\Gamma_{\mathrm{RR}}}\mathbf{H}\mathbf{t}[n] + \mathbf{v}[n] \tag{3.20}$$

where $\mathbf{t}[n]$ is the vector that represents all the signals transmitted by the relay R, and is given as:

$$\mathbf{t}[n] = \mathbf{BGr}[n-1] \tag{3.21}$$

The signal received by the destination D can now be represented by the new definitions of the parameters included and is given as:

$$y[n] = \sqrt{\Gamma_{\mathrm{RD}}}\mathbf{h}_{\mathrm{RD}}^{\mathsf{T}}\mathbf{t}[n] + \nu_D[n] \tag{3.22}$$

To simplify the mathematical operations by avoiding recursive loops in time domain, the transmitted and received signals at R and D given in (3.20), (3.21), (3.22) can be written in Z-domain as:

$$\mathbf{r}(z) = \sqrt{\Gamma_{\mathrm{SR}}}\mathbf{h}_{\mathrm{SR}}x(z) + \sqrt{\Gamma_{\mathrm{RR}}}\mathbf{H}\mathbf{t}(z) + \mathbf{v}(z) \tag{3.23}$$

$$\mathbf{t}(z) = \mathbf{BGr}(z)z^{-1} \tag{3.24}$$

$$y(z) = \sqrt{\Gamma_{\mathrm{RD}}}\mathbf{h}_{\mathrm{RD}}^{\mathsf{T}}\mathbf{t}(z) + \nu_D(z) \tag{3.25}$$

The transfer functions that were found using Mason's Gain Formula in the earlier section can now be computed in much easier manner.

3.3.1 Effective Channel for Input from S at D

The effective channel for the information bearing signal $x(z)$ from S can be computed by analyzing the input and output signals of the system. As mentioned earlier, we consider $x(z)$ to be the only input of the system and the other input signals (noise components) at R to be absent. The input signal to the relay R can be computed as follows:

$$\mathbf{r}(z) = \sqrt{\Gamma_{\mathrm{SR}}}\mathbf{h}_{\mathrm{SR}}x(z) + \sqrt{\Gamma_{\mathrm{RR}}}\mathbf{H}\mathbf{t}(z) \tag{3.26}$$

Using (3.24) in (3.26), we get

$$\begin{aligned}\mathbf{r}(z) &= \sqrt{\Gamma_{\mathrm{SR}}}\mathbf{h}_{\mathrm{SR}}x(z) + \sqrt{\Gamma_{\mathrm{RR}}}\mathbf{HBG}\mathbf{r}(z)z^{-1} \\ &= \left(\mathbf{I} - \sqrt{\Gamma_{\mathrm{RR}}}\mathbf{HBG}z^{-1}\right)^{-1}\sqrt{\Gamma_{\mathrm{SR}}}\mathbf{h}_{\mathrm{SR}}x(z) \end{aligned} \tag{3.27}$$

The signal received by D, $y(z)$ can be given as:

$$y(z) = \sqrt{\Gamma_{\mathrm{RD}}}\mathbf{h}_{\mathrm{RD}}^{\mathsf{T}}\mathbf{t}(z) \tag{3.28}$$

Using (3.24), (3.27) in (3.28),

$$\begin{aligned} y(z) &= \sqrt{\Gamma_{\mathrm{RD}}}\mathbf{h}_{\mathrm{RD}}^{\mathsf{T}}\mathbf{BG}\mathbf{r}(z)z^{-1} \\ &= \sqrt{\Gamma_{\mathrm{RD}}}\left(\mathbf{BG}\mathbf{h}_{\mathrm{RD}}\right)^{\mathsf{T}}\left(\mathbf{I}z - \sqrt{\Gamma_{\mathrm{RR}}}\mathbf{HBG}\right)^{-1}\sqrt{\Gamma_{\mathrm{SR}}}\mathbf{h}_{\mathrm{SR}}x(z) \end{aligned} \tag{3.29}$$

The transfer function with respect to the signal from source S, $H_s(z)$ is given as:

$$H_s(z) = \sqrt{\Gamma_{\mathrm{RD}}}\left(\mathbf{BG}\mathbf{h}_{\mathrm{RD}}\right)^{\mathsf{T}}\left(\mathbf{I}z - \sqrt{\Gamma_{\mathrm{RR}}}\mathbf{HBG}\right)^{-1}\sqrt{\Gamma_{\mathrm{SR}}}\mathbf{h}_{\mathrm{SR}} \tag{3.30}$$

3.3.2 Effective Channel for Noise at D

The effective channel for the noise can be computed by considering these noise components at R to be the only input signals of the system in the absence of actual information signal $x(z)$ from S. The input signal to the relay R can be found as follows:

$$\mathbf{r}(z) = \mathbf{v}(z) + \sqrt{\Gamma_{\mathrm{RR}}}\mathbf{H}\mathbf{t}(z) \tag{3.31}$$

Using (3.24) in (3.31), the input signal can be written as:

$$\begin{aligned}\mathbf{r}(z) &= \mathbf{v}(z) + \sqrt{\Gamma_{\mathrm{RR}}}\mathbf{HBG}\mathbf{r}(z)z^{-1} \\ &= \left(\mathbf{I} - \sqrt{\Gamma_{\mathrm{RR}}}\mathbf{HBG}z^{-1}\right)^{-1}\mathbf{v}(z) \end{aligned} \tag{3.32}$$

The signal received at D, $y(z)$ is same as given in (3.28), but as $r(z)$ differs, $y(z)$ also differs and is given as:

$$\begin{aligned} y(z) &= \sqrt{\Gamma_{\mathrm{RD}}}\mathbf{h}_{\mathrm{RD}}^{\mathsf{T}}\mathbf{t}(z) \\ &= \sqrt{\Gamma_{\mathrm{RD}}}\mathbf{h}_{\mathrm{RD}}^{\mathsf{T}}\mathbf{HBGr}(z)z^{-1} \\ &= \sqrt{\Gamma_{\mathrm{RD}}}\left(\mathbf{BGh}_{\mathrm{RD}}\right)^{\mathsf{T}}\left(\mathbf{I}z - \sqrt{\Gamma_{\mathrm{RR}}}\mathbf{HBG}\right)^{-1}\mathbf{v}(z) \end{aligned} \tag{3.33}$$

The transfer function with respect to the noise component $\nu_i(z)$, $H_{\nu_i}(z)$ is given as:

$$H_{\nu_i}(z) = \left[\sqrt{\Gamma_{\mathrm{RD}}}\left(\mathbf{BGh}_{\mathrm{RD}}\right)^{\mathsf{T}}\left(\mathbf{I}z - \sqrt{\Gamma_{\mathrm{RR}}}\mathbf{HBG}\right)^{-1}\right]_i \tag{3.34}$$

3.4 SUMMARY

The recursive substitution method to find the input-output relationship of the system with a full-duplex amplify-and-forward MIMO relay considered is tedious for networks that should run for longer durations. The signal flow graph approach using Mason's gain formula provides comparatively less complexity. To demonstrate this, we took an example of a 2×2 MIMO relaying system and derived the effective channel equation for both the information bearing signal input and the noise inputs. As the number of transmit and receive antennas increase at the relay, even though there are advantages in using MGF, the complexity of this approach increases and makes it less efficient. To overcome this, we introduced a new approach, using concepts of linear algebra and derived the input-output relationship of the system, effective channels for both the information signal and noise inputs for any number of antennas at the relay.

Chapter 4

PROPOSED SCHEMES AND OUTAGE PROBABILITY ANALYSIS

In this chapter, we will discuss the equalization process at the destination after the signal is received, which mitigates the effects of the interference. This will be followed by two different transmit combining techniques proposed and their analysis will be discussed in detail.

4.1 EQUALIZATION AT THE DESTINATION

As discussed in the chapters 1 and 2, full-duplex MIMO relaying systems irrespective of the processing techniques at relay are prone to the self-interference. Even though the individual channels are considered to have frequency-flat fading, the RSI makes the effective channel of the system to be frequency-selective. As a result of this RSI, the transmitted symbols are impaired by the inter-symbol interference (ISI). Methods like the Viterbi algorithm can be employed to mitigate and counter-act the effect of ISI, but as the block length of the transmitted signal is large, the implementation complexity of the Viterbi algorithm inflates abruptly. As an alternative to the efficient yet complicated Viterbi algorithm, we can use the sub-optimal technique, channel equalization to reduce the ISI, so as to mitigate the errors and enhance the reliability of the system. These equalizers can be either linear or non-linear, depending on the operations they perform. In this thesis, we consider two linear equalizers namely zero-forcing equalizer (ZFE), minimum mean squared error (MMSE) equalizer and a non-linear equalizer named minimum mean squared error decision feedback (MMSE-DFE) equalizer. It is assumed that the equalizer considered at the destina-

tion are of the infinite length that can cancel the ISI mostly and for which there are expressions to compute their output SNR.

4.1.1 Zero-forcing Equalizer (ZFE)

ZFE is a linear equalizer and is comparatively less complex than any other equalizer in terms of implementation. To mitigate the effect of ISI, the inverse of the channel's frequency response is estimated and is used as the frequency response of the linear filter through which the received signal is passed. The output SNR of the Zero-forcing equalizer is given as:

$$\gamma_{\text{ZFE}} = \left(\int_{-\frac{1}{2}}^{\frac{1}{2}} \frac{S_\nu(f)}{S_s(f)} df \right)^{-1} \tag{4.1}$$

where $S_s(f), S_\nu(f)$ are the power spectral densities with respect to the information signal and noise respectively. The major hitch in using ZFE is that, if the received signal has spectral nulls, the output SNR γ_{ZFE} turns to zero. This can be explained briefly by saying, in attempt to compensate the weak spectral frequencies, the magnitude of the gains from ZFE will be large and as a consequence, along with the signal, noise also gets enhanced by a large factor and the overall SNR get diminished. On the other hand, if the channel's frequency response itself have spectral nulls, ZFE cannot invert them at all.

4.1.2 Minimum Mean Squared Error (MMSE) Equalizer

MMSE is another type of linear equalizer which can overcome the unwanted noise enhancement that occurs with ZFE. It computes the error signal, i.e, the difference between the actual transmitted signal and the estimate of the signal and minimizes its mean square by using a filter. If e is the error signal, MMSE design constraint is

to minimize $\mathrm{E}\left[|e|^2\right]$. The output SNR of the unbiased MMSE equalizer is given as:

$$\gamma_{\text{MMSE}} = -1 + \left(\int_{-\frac{1}{2}}^{\frac{1}{2}} \frac{1}{1 + \frac{S_s(f)}{S_\nu(f)}} df \right)^{-1} \tag{4.2}$$

4.1.3 MMSE Decision Feedback Equalizer (MMSE-DFE)

The non-linear equalizers generally have a better performance than the linear equalizers but at the cost of higher implementation complexity. MMSE-DFE is one such non-linear equalizer, which consists of two filters namely a feedforward filter and a feedback filter in its structure. The signal received at the destination is fed as input to the feedforward filter and the sequence of decisions made from previous symbols are fed into the feedback filter. It is the presence of this feedback filter that makes its nature to be non-linear and more efficient, as it estimates the current symbol based on decisions made on previous symbols. The output SNR of the unbiased MMSE-DFE equalizer is given as:

$$\gamma_{\text{MMSE-DFE}} = -1 + \exp\left(\int_{-\frac{1}{2}}^{\frac{1}{2}} \ln\left(1 + \frac{S_s(f)}{S_\nu(f)}\right) df \right) \tag{4.3}$$

The power spectral densities $S_s(f), S_\nu(f)$ can be found from the transfer functions derived in chapter 2 and upon substituting them into (4.1), (4.2), (4.3), we can find the output SNR of the respective equalizers. Alternatively, we can say that the output SNR of the equalizer is a function of the channel realizations and can be found by using the above given expressions. If the resulting SNR is found to be below a pre-determined threshold SNR Γ_T, we consider that there is an outage for the end-to-end system. This threshold SNR Γ_T is derived from the target rate of the system, R_T, given by the Shannon capacity formula as,

$$R_T = \log_2\left(1 + \Gamma_T\right) \text{bps/Hz} \tag{4.4}$$

4.2 EQUAL GAIN TRANSMISSION

As discussed in chapter 2, though it is conspicuous that MRC is superior to any other combining technique, we can also manifest that it has a higher implementation complexity as the relay needs to have information about both the magnitude and phase of the channels. Whereas, EGC, although is next to MRC in performance,

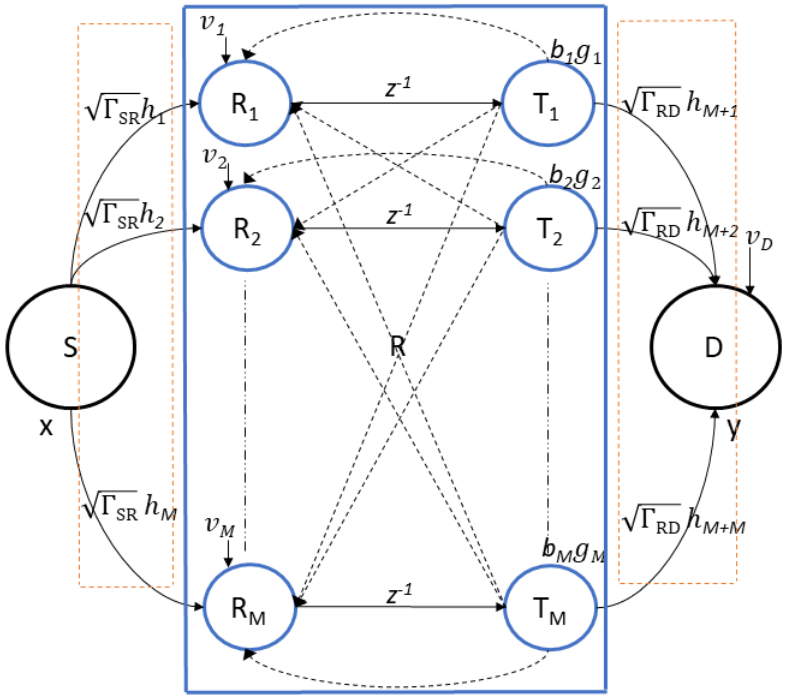

Figure 4.1: Block Diagram for a system with Equal-Gain Transmission at $M \times M$ FD AF Relay

needs only the information about the phase of the channels and thus reducing the complexity. However, in this thesis, the system model has multiple antennas at the relay and not at the destination. Hence, we use this equal gain combining technique at the transmitter i.e., relay R and we call it Equal Gain Transmission (EGT). When compared to its contender maximal ratio transmission (MRT), in MRT, the perfor-

mance is at its best if the per-antenna power allocation is dynamic depending on the channel strength, whereas, in EGT, the total transmit power at the relay is equally shared among all its transmitting antennas, irrespective of the channel strengths. The signals received and transmitted by relay and the signal at D are given by (3.20), (3.21), (3.22).

4.2.1 Amplification Gain at the Relay

We assume that, both the source, S and relay, R transmit signals $x[n]$ and $\mathbf{t}[n]$ at normalized average power of unity, i.e.,

$$\mathrm{E}\left[\left|x[n]\right|^2\right] = \mathrm{E}\left[\left\|\mathbf{t}[n]\right\|^2\right] = 1 \tag{4.5}$$

where $\mathrm{E}[.]$ denotes the average over signal and noise distributions. As the total power at R is normalized, without loss of generality, the average power at each antenna is considered to be $\mathrm{E}\left[\left|t_i[n]\right|^2\right] = \frac{1}{M}$. The relay R receives signal $r_i[n]$ at each R_i given by (3.1), which are copies of the signal $x[n]$, transmitted by S. After amplifying the received signal, with a processing delay of one symbol, R transmits signal $t_i[n]$ from each T_i given by (3.2). To find the amplification factor g_i at T_i, we perform recursive substitution of (3.1) into (3.2):

$$\begin{aligned}
t_i[n] &= b_i g_i r_i[n-1] \\
&= b_i g_i \Bigg(\sqrt{\Gamma_{\mathrm{SR}}} h_i x[n-1] + \sqrt{\Gamma_{\mathrm{RR}}} \left(h_{1i} t_1[n-1] + h_{2i} t_2[n-1] + ... + h_{Mi} t_M[n-1] \right) \\
&\qquad\qquad + \nu_i[n-1] \Bigg) \\
&= b_i g_i \left(\sqrt{\Gamma_{\mathrm{SR}}} h_i x[n-1] + \sqrt{\Gamma_{\mathrm{RR}}} \sum_{j=1}^{M} h_{ji} t_j[n-1] + \nu_i[n-1] \right)
\end{aligned} \tag{4.6}$$

The instantaneous transmit power per antenna can be calculated using (4.6) to be,

$$\mathrm{E}\left[\left|t_i[n]\right|^2\right] = |b_i g_i|^2 \Bigg(\Gamma_{\mathrm{SR}} \left|h_i\right|^2 \mathrm{E}\left[\left|x[n-1]\right|^2\right] + \Gamma_{\mathrm{RR}} \sum_{j=1}^{M} \left|h_{ji}\right|^2 \mathrm{E}\left[\left|t_j[n-1]\right|^2\right] + \mathrm{E}\left[\left|\nu_i[n-1]\right|^2\right] \Bigg)$$

$$\frac{1}{M} = |b_i g_i|^2 \left(\Gamma_{\mathrm{SR}} \left|h_i\right|^2 + \frac{\Gamma_{\mathrm{RR}}}{M} \sum_{j=1}^{M} \left|h_{ji}\right|^2 + \sigma_\nu^2 \right)$$

$$g_i = \frac{1}{|b_i|} \left(M\Gamma_{\mathrm{SR}} \left|h_i\right|^2 + \Gamma_{\mathrm{RR}} \sum_{j=1}^{M} \left|h_{ji}\right|^2 + M \right)^{-1/2} \tag{4.7}$$

where $\sigma_\nu^2 = 1$. (4.7) gives us the amplification factor at each T_i of R, assuming that the total transmit power of R is normalized to average power of unity. These g_is are combined together in a diagonal matrix form $\mathbf{G}$ as shown in (3.18).

4.2.2 Pre-coding Matrix at Relay

In equal gain transmission, we aim to transmit the signals with equal gain and cancel the phase at each T_i of the relay. Equal gain coefficients are shown in the previous section. In this section, we will talk about the co-phasing parameters.

To co-phase the channels over the transmitted signal, we define pre-coding parameter b_i, such that it cancels the phase due to channels behind the relay, i.e., phase of $\mathbf{h}_{\mathrm{SR}}$ and phase due to the channels ahead of the relay, i.e., phase of $\mathbf{h}_{\mathrm{RD}}$. The pre-coding parameter b_i is given as :

$$b_i = e^{-j\left(\angle h_i + \angle h_{M+i}\right)} \tag{4.8}$$

The b_is are combined together in a diagonal matrix form $\mathbf{B}$ as shown in (3.19). The received signal at D can be elaboratively written as:

$$y[n] = \underbrace{\sqrt{\Gamma_{\mathrm{SR}}\Gamma_{\mathrm{RD}}}\sum_{i=1}^{M} h_i h_{M+i} b_i g_i x[n-1]}_{\text{Signal}} + \underbrace{\sqrt{\Gamma_{\mathrm{RR}}\Gamma_{\mathrm{RD}}}\sum_{i=1}^{M} h_{M+i} b_i g_i \sum_{j=1}^{M} h_{ji} t_j[n-1] + \sqrt{\Gamma_{\mathrm{RD}}}\sum_{i=1}^{M} h_{M+i} b_i g_i \nu_i[n-1] + \nu_D[n]}_{\text{RSI + Noise}} \quad (4.9)$$

From the above equation, we can easily compute the SNR at D for the received signal and is given by:

$$\mathrm{SNR} = \frac{\left|\sqrt{\Gamma_{\mathrm{SR}}\Gamma_{\mathrm{RD}}}\sum_{i=1}^{M} h_i h_{M+i} b_i g_i\right|^2}{\left|\sqrt{\Gamma_{\mathrm{RR}}\Gamma_{\mathrm{RD}}}\sum_{i=1}^{M}\sum_{j=1}^{M} h_{M+i} h_{ji} b_i g_i\right|^2 + \left|\sqrt{\Gamma_{\mathrm{RD}}}\sum_{i=1}^{M} h_{M+i} b_i g_i\right|^2 + 1} \quad (4.10)$$

The effective channels for signal from S and noise components are same as the ones derived in chapter 3, given in equations (3.30), (3.34). As mentioned earlier, we assume that all the noise components at the receiving antennas of the relay to be independent, we can derive the power spectral densities of the signal $S_s(f)$ and the noise $S_{\nu_i}(f)$ from (3.30), (3.34) by converting the Z-domain to Fourier domain $\left(z = e^{j2\pi f}\right)$ as shown below:

$$\begin{aligned} S_s(f) &= \left|H_s\left(e^{j2\pi f}\right)\right|^2 \\ &= \left|\sqrt{\Gamma_{\mathrm{RD}}}\left(\mathbf{B}\mathbf{G}\mathbf{h}_{\mathrm{RD}}\right)^{\mathsf{T}}\left(\mathbf{I}e^{j2\pi f} - \sqrt{\Gamma_{\mathrm{RR}}}\mathbf{H}\mathbf{B}\mathbf{G}\right)^{-1}\sqrt{\Gamma_{\mathrm{SR}}}\mathbf{h}_{\mathrm{SR}}\right|^2 \end{aligned} \quad (4.11)$$

$$\begin{aligned} S_{\nu_i}(f) &= \left|H_{\nu_i}\left(e^{j2\pi f}\right)\right|^2 \\ &= \left|\left[\sqrt{\Gamma_{\mathrm{RD}}}\left(\mathbf{B}\mathbf{G}\mathbf{h}_{\mathrm{RD}}\right)^{\mathsf{T}}\left(\mathbf{I}e^{j2\pi f} - \sqrt{\Gamma_{\mathrm{RR}}}\mathbf{H}\mathbf{B}\mathbf{G}\right)^{-1}\right]_i\right|^2 \end{aligned} \quad (4.12)$$

Overall power spectral density of the noise inputs at all the receiving antennas of R, $S_\nu(f)$, can be derived as follows:

$$\begin{aligned} S_\nu(f) &= \sigma_\nu^2 \left[1 + \sum_{i=1}^{N} S_{\nu_i}(f)\right] \\ &= 1 + \left\| \sqrt{\Gamma_{\mathrm{RD}}} \left(\mathbf{BGh}_{\mathrm{RD}}\right)^{\mathsf{T}} \left(\mathbf{I}e^{j2\pi f} - \sqrt{\Gamma_{\mathrm{RR}}}\mathbf{HBG}\right)^{-1} \right\|^2 \end{aligned} \tag{4.13}$$

Using the power spectral densities given in (4.11), (4.13) we can find the end-to-end SNR of the system by substituting these in the equalizer SNR expressions presented in the section 4.1.

4.3 ANTENNA SELECTION

We have discussed the selection combining (SC) technique in chapter 2. The antenna selection (AS) scheme can be related to SC, the only difference being, in AS, we choose the transmit-receive antenna pair at R to transmit and receive as per some selection criterion. In this scheme, at any point of time during the transmission, only one pair of transmit-receive antennas $(\mathrm{T}_i, \mathrm{R}_i)$ is active at the relay R. Although, one can come up with many selection criteria, in this thesis we will discuss four particular criteria:

- **AS1**:Choosing $\mathrm{T}_i, \mathrm{R}_i$ pair which has maximum $|h_i h_{M+i}|$ product.
- **AS2**:Choosing $\mathrm{T}_i, \mathrm{R}_i$ pair which has maximum SNR at the input of the equalizer
- **AS3**:Choosing $\mathrm{T}_i, \mathrm{R}_i$ pair which has maximum SNR at the input of the equalizer without having any knowledge about the RSI channels
- **AS4**:Choosing $\mathrm{T}_i, \mathrm{R}_i$ pair which has maximum SNR at the output of the equalizer

Each of these criteria will be discussed in detail and their analysis will be shown further. In this antenna selection scheme, to make things simple, we consider the pre-coding parameter b_i to be 1 and assume the co-phasing can be done at the destination, which doesn't show any effect in the overall performance. Assuming that the i^{th}

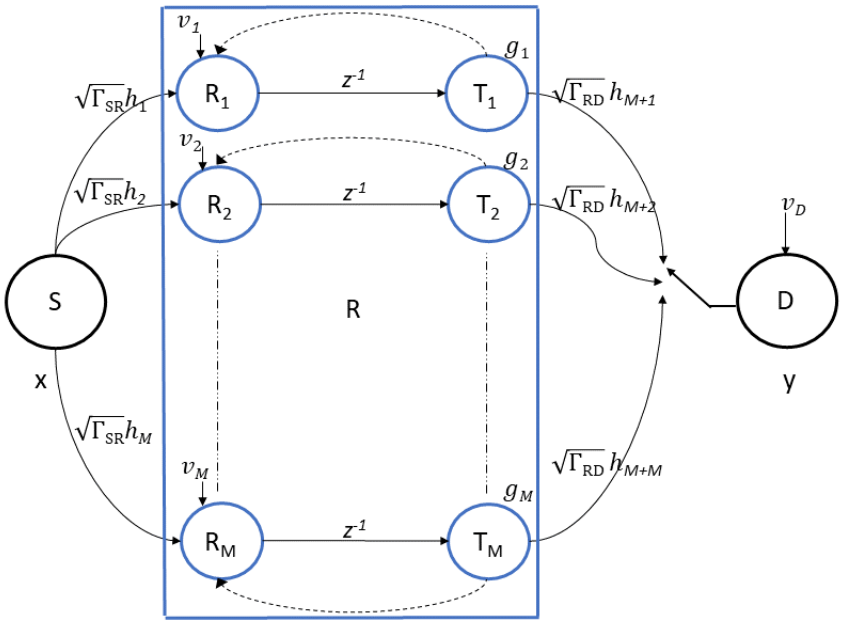

Figure 4.2: Block Diagram for a system with Antenna Selection at $M \times M$ FD AF Relay

antenna pair is selected, the received signal at relay R, $r_i[n]$ has three components same as in EGT, which are the signal $x[n]$ from S, self-interference component and the additive Gaussian noise.

$$r_i[n] = \sqrt{\Gamma_{SR}}h_i x[n] + \sqrt{\Gamma_{RR}}h_{ii}t_i[n] + \nu_i[n] \tag{4.14}$$

As mentioned earlier, assuming processing delay of a symbol period, the transmitted signal at R, $t_i[n]$ is given as:

$$t_i[n] = g_i r_i[n-1] \tag{4.15}$$

4.3.1 Amplification Factor at Relay

Similar to equal gain transmission technique, we assume that, both the source, S and the relay, R, transmit signals $x[n]$ and $t_i[n]$ at normalized average power of unity, i.e.,

$$\mathrm{E}\left[\left|x[n]\right|^2\right] = \mathrm{E}\left[\left|t_i[n]\right|^2\right] = 1 \tag{4.16}$$

In EGT, the total transmit power is shared equally among M transmit antennas, whereas in AS, as it is only one antenna transmitting at any time, the total power available at relay R is allocated to that selected transmit antenna. Substituting (4.14) in (4.15),

$$t_i[n] = g_i\left(\sqrt{\Gamma_{\mathrm{SR}}}h_i x[n-1] + \sqrt{\Gamma_{\mathrm{RR}}}h_{ii}t_i[n-1] + \nu_i[n-1]\right) \tag{4.17}$$

The instantaneous transmit power at relay R can be computed using (4.17) as:

$$\begin{aligned}
\mathrm{E}\left[\left|t_i[n]\right|^2\right] &= |g_i|^2\left(\Gamma_{\mathrm{SR}}\left|h_i\right|^2 + \Gamma_{\mathrm{RR}}\left|h_{ii}\right|^2 + \sigma_\nu^2\right) \\
1 &= |g_i|^2\left(\Gamma_{\mathrm{SR}}\left|h_i\right|^2 + \Gamma_{\mathrm{RR}}\left|h_{ii}\right|^2 + 1\right) \\
g_i &= \left(\Gamma_{\mathrm{SR}}\left|h_i\right|^2 + \Gamma_{\mathrm{RR}}\left|h_{ii}\right|^2 + 1\right)^{-1/2}
\end{aligned} \tag{4.18}$$

(4.18) gives us the amplification factor g_i at R for the AS scheme.

Now, as the relay amplifies and forwards using only one of the antenna pairs, the received signal at the final destination D, $y[n]$ comprises of the three components which are the desired signal from source S, the unwanted RSI component and the

noise and this is shown in the equation 4.19 given below.

$$\begin{aligned} y[n] &= \sqrt{\Gamma_{\mathrm{RD}}} h_{M+i} t_i[n] + \nu_D[n] \\ &= \sqrt{\Gamma_{\mathrm{RD}}} h_{M+i} \left(g_i \left(\sqrt{\Gamma_{\mathrm{SR}}} h_i x[n-1] + \sqrt{\Gamma_{\mathrm{RR}}} h_{ii} t_i[n-1] + \nu_i[n-1] \right) \right) + \nu_D[n] \\ &= \underbrace{\sqrt{\Gamma_{\mathrm{SR}}\Gamma_{\mathrm{RD}}} h_i h_{M+i} g_i x[n-1]}_{\text{Signal}} + \underbrace{\sqrt{\Gamma_{\mathrm{RR}}\Gamma_{\mathrm{RD}}} h_{ii} h_{M+i} g_i t_i[n-1]}_{\text{RSI}} \\ &\qquad + \underbrace{\sqrt{\Gamma_{\mathrm{RD}}} h_{M+i} g_i \nu_i[n-1] + \nu_D[n]}_{\text{Noise}} \end{aligned} \tag{4.19}$$

Selection Criterion 1 (AS1):

In this criterion, the channel gains between S-R and R-D are only taken into account and their product is found at all the transmit-receive antenna pairs and the best among them is chosen. As only the selected pair will be kept active until the channels change i.e., for the duration of coherence time. D, receives the signal from T_i and is same as given in (4.19). The AS1 selection criterion can be given as:

$$\underset{1 \le i \le M}{\arg\max} \left(|h_i h_{M+i}| \right) \tag{4.20}$$

Selection Criterion 2 (AS2):

Here, we compute the SNR at D, from the received signal given in (4.19) before equalization for all the antenna pairs and the best among them is chosen. The corresponding antenna pair will be kept active for the duration of coherence time and the process keeps repeating every time the channel changes. The AS2 selection criterion is given by:

$$\underset{1 \le i \le M}{\arg\max} \left(\frac{\left| \sqrt{\Gamma_{\mathrm{SR}}\Gamma_{\mathrm{RD}}} h_i h_{M+i} g_i \right|^2}{\left| \sqrt{\Gamma_{\mathrm{RR}}\Gamma_{\mathrm{RD}}} h_{ii} h_{M+i} g_i \right|^2 + \left| \sqrt{\Gamma_{\mathrm{RD}}} h_{M+i} g_i \right|^2 + 1} \right) \tag{4.21}$$

Selection Criterion 3 (AS3):

The selection criterion AS2 requires knowledge of the RSI channels to make a decision on which pair of antennas should transmit. As it is difficult to attain the knowledge of the RSI at relay, we propose another strategy, where the relay does not need to have any kind of knowledge of the RSI channels to make the decision. We ignore the interference component presented in the AS2 criterion and the new criterion AS3 can be given by:

$$\underset{1\leq i\leq M}{\arg\max}\left(\frac{\left|\sqrt{\Gamma_{\mathrm{SR}}\Gamma_{\mathrm{RD}}}h_i h_{M+i} g_i\right|^2}{\left|\sqrt{\Gamma_{\mathrm{RD}}}h_{M+i} g_i\right|^2+1}\right) \tag{4.22}$$

Selection Criterion 4 (AS4):

Similar to AS2, here also we compute the SNR at D, corresponding to the signal received from all the antenna pairs, but only at the output of the equalizer. For any of the equalizers discussed in section 4.1, the corresponding SNRs given in (4.1),(4.2),(4.3) are computed and the best among all the antenna pairs is chosen and the respective pair is kept active for transmission. Assuming that the destination deploys MMSE-DFE equalizer, the selection criterion can be given as:

$$\underset{1\leq i\leq M}{\arg\max}\left(-1+\exp\left(\int_{-0.5}^{0.5}\ln\left(1+\frac{\left|\sqrt{\Gamma_{\mathrm{SR}}\Gamma_{\mathrm{RD}}}h_i h_{M+i} g_i\right|^2}{\left|e^{j2\pi f}-\sqrt{\Gamma_{\mathrm{RR}}}h_{ii} g_i\right|^2+\left|\sqrt{\Gamma_{\mathrm{RD}}}h_{M+i} g_i\right|^2}\right)df\right)\right) \tag{4.23}$$

4.3.2 Effective Channel for Input from S at D

The effective channel for the actual information signal $x(z)$ from S. We consider the presence of $x(z)$ as the only input signal and the other noise components are

absent. The input signal at R, in transform domain, $r_i(z)$, is given as:

$$\begin{aligned} r_i(z) &= \sqrt{\Gamma_{\mathrm{SR}}} h_i x(z) + \sqrt{\Gamma_{\mathrm{RR}}} h_{ii} t_i(z) \\ &= \sqrt{\Gamma_{\mathrm{SR}}} h_i x(z) + \sqrt{\Gamma_{\mathrm{RR}}} h_{ii} g_i r_i(z) z^{-1} \\ &= \left(1 - \sqrt{\Gamma_{\mathrm{RR}}} h_{ii} g_i z^{-1}\right)^{-1} \sqrt{\Gamma_{\mathrm{SR}}} h_i x(z) \end{aligned} \tag{4.24}$$

In the absence of noise, the received signal at D, given in (4.19) can be rewritten in transform domain using (4.24) as shown below:

$$\begin{aligned} y(z) &= \sqrt{\Gamma_{\mathrm{RD}}} h_{M+i} t_i(z) \\ &= \sqrt{\Gamma_{\mathrm{RD}}} h_{M+i} g_i r_i(z) z^{-1} \\ &= \sqrt{\Gamma_{\mathrm{SR}} \Gamma_{\mathrm{RD}}} h_i h_{M+i} g_i \left(z - \sqrt{\Gamma_{\mathrm{RR}}} h_{ii} g_i\right)^{-1} x(z) \end{aligned} \tag{4.25}$$

The overall transfer function with respect to the signal from S can be written as below:

$$H_s(z) = \sqrt{\Gamma_{\mathrm{SR}} \Gamma_{\mathrm{RD}}} h_i h_{M+i} g_i \left(z - \sqrt{\Gamma_{\mathrm{RR}}} h_{ii} g_i\right)^{-1} \tag{4.26}$$

4.3.3 Effective Channel for Noise at D

The effective channel for noise inputs at the relay R can be computed by considering this noise component as the only input and the signal from S is absent. The input signal at R, in transform-domain, $r_i(z)$ is given as:

$$\begin{aligned} r_i(z) &= \nu_i(z) + \sqrt{\Gamma_{\mathrm{RR}}} h_{ii} t_i(z) \\ &= \nu_i(z) + \sqrt{\Gamma_{\mathrm{RR}}} h_{ii} g_i r_i(z) z^{-1} \\ &= \left(1 - \sqrt{\Gamma_{\mathrm{RR}}} h_{ii} g_i z^{-1}\right)^{-1} \nu_i(z) \end{aligned} \tag{4.27}$$

The received signal at destination D can be given by:

$$\begin{aligned} y(z) &= \sqrt{\Gamma_{\mathrm{RD}}} h_{M+i} t_i(z) \\ &= \sqrt{\Gamma_{\mathrm{RD}}} h_{M+i} g_i r_i(z) z^{-1} \\ &= \sqrt{\Gamma_{\mathrm{RD}}} h_{M+i} g_i \left(z - \sqrt{\Gamma_{\mathrm{RR}}} h_{ii} g_i \right)^{-1} \nu_i(z) \end{aligned} \tag{4.28}$$

The transfer function with respect to the noise component as input can be written as below:

$$H_\nu(z) = \sqrt{\Gamma_{\mathrm{RD}}} h_{M+i} g_i \left(z - \sqrt{\Gamma_{\mathrm{RR}}} h_{ii} g_i \right)^{-1} \tag{4.29}$$

The power spectral densities of the signal $S_s(f)$ and the noise $S_\nu(f)$ from (4.26) and (4.29) can be derived the same way as we did in EGT and are shown below.

$$S_s(f) = \left| H_s \left(e^{j2\pi f} \right) \right|^2 = \frac{\left| \sqrt{\Gamma_{\mathrm{SR}} \Gamma_{\mathrm{RD}}} h_i h_{M+i} g_i \right|^2}{\left| e^{j2\pi f} - \sqrt{\Gamma_{\mathrm{RR}}} h_{ii} g_i \right|^2} \tag{4.30}$$

$$S_\nu(f) = \sigma_\nu^2 \left[1 + \left| H_\nu \left(e^{j2\pi f} \right) \right|^2 \right] = 1 + \frac{\left| \sqrt{\Gamma_{\mathrm{RD}}} h_{M+i} g_i \right|^2}{\left| e^{j2\pi f} - \sqrt{\Gamma_{\mathrm{RR}}} h_{ii} g_i \right|^2} \tag{4.31}$$

Using these spectral densities, one can find the overall SNR of the system for any selection criterion, by using the output SNR expressions for any of the equalizers discussed and the corresponding outage probabilities are computed.

4.4 BOUND FOR OUTAGE PROBABILITY OF ANTENNA SELECTION

To check the performance of the proposed antenna selection technique, we propose a bound for the outage probability of the scheme. We consider the presence of an unbiased MMSE-DFE equalizer at D, assuming no error propagation during the equalization, the output SNR is given by (4.3). The ratio of the power spectral

densities given in (4.30), (4.31) is given by:

$$\begin{aligned}\frac{S_s(f)}{S_\nu(f)} &= \frac{\left|\sqrt{\Gamma_{\text{SR}}\Gamma_{\text{RD}}}h_i h_{M+i} g_i\right|^2}{\left|e^{j2\pi f} - \sqrt{\Gamma_{\text{RR}}}h_{ii}g_i\right|^2 + \left|\sqrt{\Gamma_{\text{RD}}}h_{M+i}g_i\right|^2} \\ &= \frac{g_i^2\Gamma_{\text{SR}}\Gamma_{\text{RD}}\left|h_i\right|^2\left|h_{M+i}\right|^2}{1+\Gamma_{\text{RR}}g_i^2\left|h_{ii}\right|^2 - 2\text{Re}\left\{e^{-j2\pi f}\sqrt{\Gamma_{\text{RR}}}g_i h_{ii}\right\} + g_i^2\Gamma_{\text{RD}}\left|h_{M+i}\right|^2} \\ &= \frac{\Gamma_{\text{SR}}\Gamma_{\text{RD}}\left|h_i\right|^2\left|h_{M+i}\right|^2}{\frac{1}{g_i^2}+\Gamma_{\text{RR}}\left|h_{ii}\right|^2 - \frac{2\sqrt{\Gamma_{\text{RR}}}}{g_i}\text{Re}\left\{e^{-j2\pi f}r_{ii}e^{j\theta}\right\} + \Gamma_{\text{RD}}\left|h_{M+i}\right|^2} \\ &= \frac{\Gamma_{\text{SR}}\Gamma_{\text{RD}}\left|h_i\right|^2\left|h_{M+i}\right|^2}{1+\Gamma_{\text{SR}}\left|h_i\right|^2+\Gamma_{\text{RD}}\left|h_{M+i}\right|^2+2\Gamma_{\text{RR}}\left|h_{ii}\right|^2 - C} \end{aligned} \tag{4.32}$$

where, $C = 2\sqrt{\Gamma_{\text{RR}}\left(\Gamma_{\text{SR}}\left|h_i\right|^2+\Gamma_{\text{RR}}\left|h_{ii}\right|^2+1\right)}r_{ii}\cos(2\pi f-\theta)$

Using (4.32) in (4.3), output SNR, $\gamma_{\text{MMSE-DFE}}$ can be found to be

$$\gamma_{\text{MMSE-DFE}} = -1 + \exp\left(\int_{-\frac{1}{2}}^{\frac{1}{2}} \ln\left(\frac{B+A}{B}\right)df\right) \tag{4.33}$$

where

$$A = \Gamma_{\text{SR}}\Gamma_{\text{RD}}\left|h_i\right|^2\left|h_{M+i}\right|^2 \tag{4.34}$$

$$B = 1+\Gamma_{\text{SR}}\left|h_i\right|^2+\Gamma_{\text{RD}}\left|h_{M+i}\right|^2+2\Gamma_{\text{RR}}\left|h_{ii}\right|^2 - C \tag{4.35}$$

With the help of [75], the exponent in (4.33) can be simplified to get,

$$\begin{aligned}\gamma_{\text{MMSE-DFE}} &= -1 + \frac{Q_1+\sqrt{Q_1^2-Q_3^2}}{Q_2+\sqrt{Q_2^2-Q_3^2}} \\ &= \frac{\Gamma_{\text{SR}}\Gamma_{\text{RD}}\left|h_i\right|^2\left|h_{M+i}\right|^2+\sqrt{Q_1^2-Q_3^2}+\sqrt{Q_2^2-Q_3^2}}{Q_2+\sqrt{Q_2^2-Q_3^2}} \\ &\geq \frac{\Gamma_{\text{SR}}\Gamma_{\text{RD}}\left|h_i\right|^2\left|h_{M+i}\right|^2}{1+\Gamma_{\text{SR}}\left|h_i\right|^2+\Gamma_{\text{RD}}\left|h_{M+i}\right|^2+2\Gamma_{\text{RR}}\left|h_{ii}\right|^2} \end{aligned} \tag{4.36}$$

where

$$Q_1 = 1+\Gamma_{\text{SR}}\left|h_i\right|^2+\Gamma_{\text{RD}}\left|h_{M+i}\right|^2+2\Gamma_{\text{RR}}\left|h_{ii}\right|^2+\Gamma_{\text{SR}}\Gamma_{\text{RD}}\left|h_i\right|^2\left|h_{M+i}\right|^2$$

$$Q_2 = 1+\Gamma_{\text{SR}}\left|h_i\right|^2+\Gamma_{\text{RD}}\left|h_{M+i}\right|^2+2\Gamma_{\text{RR}}\left|h_{ii}\right|^2$$

$$Q_3 = -2r_{ii}\sqrt{\Gamma_{\text{RR}}(\Gamma_{\text{SR}}\left|h_i\right|^2+\Gamma_{\text{RR}}\left|h_{ii}\right|^2+1)}$$

We need to keep a note that as all the channels are designed to be Rayleigh faded, with variance unity, the random variables $|h_i|^2, |h_{M+i}|^2, |h_{ii}|^2$ will be exponential random variables with mean 1. The outage probability is bounded by:

$$\Pr\left(\gamma_{\text{MMSE-DFE}} \leq \Gamma_T\right) \leq$$

$$\left(\Pr\left(\frac{\Gamma_{\text{SR}}\Gamma_{\text{RD}}\left|h_i\right|^2\left|h_{M+i}\right|^2}{1+\Gamma_{\text{SR}}\left|h_i\right|^2+\Gamma_{\text{RD}}\left|h_{M+i}\right|^2+2\Gamma_{\text{RR}}\left|h_i\right|^2} \leq \Gamma_T\right)\right)^M$$

$$= \left(\Pr\left(\Gamma_{\text{RR}}\left|h_{ii}\right|^2 \geq \frac{\Gamma_{\text{SR}}\Gamma_{\text{RD}}|h_i|^2|h_{M+i}|^2 - \Gamma_T(1+\Gamma_{\text{SR}}|h_i|^2+\Gamma_{\text{RD}}|h_{M+i}|^2)}{2\Gamma_T}\right)\right)^M$$

$$= \left(1-\Pr\left(|h_{ii}|^2 \leq \underbrace{\frac{1}{2\Gamma_T\Gamma_{\text{RR}}}\left(\Gamma_{\text{SR}}|h_i|^2(\Gamma_{\text{RD}}|h_{M+i}|^2-\Gamma_T)-\Gamma_T(1+\Gamma_{\text{RD}}|h_{M+i}|^2)\right)}_{\Psi}\right)\right)^M$$

$$= \left(1-\iint_{\Psi\geq 0}\left(1-e^{-\Psi}\right)e^{-|h_i|^2}e^{-\left|h_{M+i}\right|^2}d\left|h_i\right|^2 d\left|h_{M+i}\right|^2\right)^M \tag{4.37}$$

We can divide the integration region $\Psi \geq 0$ with integration limits $\alpha \leq \left|h_{M+i}\right|^2 < \infty$ and $\beta \leq |h_i|^2 < \infty$, where $\alpha = \frac{\Gamma_T}{\Gamma_{\text{RD}}}, \beta = \frac{\Gamma_T\left(1+\Gamma_{\text{RD}}\left|h_{M+i}\right|^2\right)}{\Gamma_{\text{SR}}\left(\Gamma_{\text{RD}}\left|h_{M+i}\right|^2-\Gamma_T\right)}$

$$\Pr\left(\gamma_{\text{MMSE-DFE}} \leq \Gamma_T\right)$$

$$\leq \left(1-\int_{\left|h_{M+i}\right|^2=\alpha}^{\infty}\int_{|h_i|^2=\beta}^{\infty}\left(1-e^{-\Psi}\right)e^{-|h_i|^2}e^{-\left|h_{M+i}\right|^2}d\left|h_i\right|^2 d\left|h_{M+i}\right|^2\right)^M \tag{4.38}$$

Let us consider the RHS of (4.38) and simplify it further.

$$
\begin{aligned}
&\left(1-\int_{\left|h_{M+i}\right|^2=\alpha}^{\infty}\int_{|h_i|^2=\beta}^{\infty}\left(1-e^{-\Psi}\right)e^{-|h_i|^2}e^{-\left|h_{M+i}\right|^2}d\left|h_i\right|^2 d\left|h_{M+i}\right|^2\right)^M\\
&=\left(1-\int_{\left|h_{M+i}\right|^2=\alpha}^{\infty}e^{-\left|h_{M+i}\right|^2}\int_{|h_i|^2=\beta}^{\infty}\left(1-e^{-\Psi}\right)e^{-|h_i|^2}d\left|h_i\right|^2 d\left|h_{M+i}\right|^2\right)^M\\
&=\Bigg(1-\int_{\left|h_{M+i}\right|^2=\alpha}^{\infty}e^{-\left|h_{M+i}\right|^2}\Bigg(\int_{|h_i|^2=\beta}^{\infty}e^{-|h_i|^2}d\left|h_i\right|^2-\\
&\qquad\qquad\int_{|h_i|^2=\beta}^{\infty}e^{-\left(\Psi+|h_i|^2\right)}d\left|h_i\right|^2\Bigg)d\left|h_{M+i}\right|^2\Bigg)^M\\
&=\left(1-\int_{\left|h_{M+i}\right|^2=\alpha}^{\infty}e^{-\left|h_{M+i}\right|^2}\left(e^{-\beta}-\frac{e^{-\beta}}{1+\frac{\Gamma_{\mathrm{SR}}\left(\Gamma_{\mathrm{RD}}\left|h_{M+i}\right|^2-\Gamma_T\right)}{2\Gamma_T\Gamma_{\mathrm{RR}}}}\right)d|h_{M+i}|^2\right)^M\\
&=\left(1-\int_{\left|h_{M+i}\right|^2=\alpha}^{\infty}e^{-|h_{M+i}|^2-\beta}\left(\frac{2\Gamma_T\Gamma_{\mathrm{RR}}+\Gamma_{\mathrm{SR}}\left(\Gamma_{\mathrm{RD}}\left|h_{M+i}\right|^2-\Gamma_T\right)-2\Gamma_T\Gamma_{\mathrm{RR}}}{2\Gamma_T\Gamma_{\mathrm{RR}}+\Gamma_{\mathrm{SR}}\left(\Gamma_{\mathrm{RD}}\left|h_{M+i}\right|^2-\Gamma_T\right)}\right)\right)^M\\
&=\left(1-\int_{z=0}^{\infty}\frac{\Gamma_{\mathrm{SR}}z}{\Gamma_{\mathrm{SR}}z+2\Gamma_T\Gamma_{\mathrm{RR}}}e^{-\left(\frac{\Gamma_T+z}{\Gamma_{\mathrm{RD}}}\right)}e^{-\frac{\Gamma_T\left(1+\Gamma_T+z\right)}{\Gamma_{\mathrm{SR}}z}}\frac{1}{\Gamma_{\mathrm{RD}}}dz\right)^M\\
&=\left(1-\frac{1}{\Gamma_{\mathrm{RD}}}e^{-\frac{\Gamma_T}{\Gamma_{\mathrm{RD}}}}e^{-\frac{\Gamma_T}{\Gamma_{\mathrm{SR}}}}\int_{z=0}^{\infty}\frac{\Gamma_{\mathrm{SR}}z}{\Gamma_{\mathrm{SR}}z+2\Gamma_T\Gamma_{\mathrm{RR}}}e^{-\frac{z}{\Gamma_{\mathrm{RD}}}}e^{-\frac{\Gamma_T(1+\Gamma_T)}{\Gamma_{\mathrm{SR}}z}}dz\right)^M
\end{aligned}
\tag{4.39}
$$

where, $z=\Gamma_{\mathrm{RD}}\left|h_{M+i}\right|^2-\Gamma_T$. Let us consider two cases for moderate RSI and strong RSI at R. First, when $\frac{2\Gamma_{\mathrm{RR}}\Gamma_T}{\Gamma_{\mathrm{SR}}\Gamma_{\mathrm{RD}}}\ll 1$, i.e., we have a relatively moderate RSI, we approximate $\frac{\Gamma_{\mathrm{SR}}z}{\Gamma_{\mathrm{SR}}z+2\Gamma_T\Gamma_{\mathrm{RR}}}\simeq 1-\frac{2\Gamma_{\mathrm{RR}}\Gamma_T}{\Gamma_{\mathrm{SR}}z}$. Combining this with (4.39), and applying

Eq.3.471.9 from [75], we can see,

$$\begin{aligned}
&\Pr\left(\gamma_{\text{MMSE-DFE}} \leq \Gamma_T\right) \\
&\leq \left(1 - \frac{1}{\Gamma_{\text{RD}}} e^{-\frac{\Gamma_T}{\Gamma_{\text{RD}}}} e^{-\frac{\Gamma_T}{\Gamma_{\text{SR}}}} \int_{z=0}^{\infty} e^{-\frac{z}{\Gamma_{\text{RD}}}} e^{-\frac{\Gamma_T(1+\Gamma_T)}{\Gamma_{\text{SR}} z}} \left(1 - \frac{2\Gamma_T \Gamma_{\text{RR}}}{\Gamma_{\text{SR}} z}\right) dz\right)^M \\
&\approx \left(1 - \frac{1}{\Gamma_{\text{RD}}} e^{-\frac{\Gamma_T}{\Gamma_{\text{RD}}}} e^{-\frac{\Gamma_T}{\Gamma_{\text{SR}}}} \left(\int_{z=0}^{\infty} e^{-\frac{\Gamma_T(1+\Gamma_T)}{\Gamma_{\text{SR}} z} - \frac{z}{\Gamma_{\text{RD}}}} dz - \int_{z=0}^{\infty} \frac{2\Gamma_T \Gamma_{\text{RR}}}{\Gamma_{\text{SR}}} z^{-1} e^{-\frac{\Gamma_T(1+\Gamma_T)}{\Gamma_{\text{SR}} z} - \frac{z}{\Gamma_{\text{RD}}}} dz\right)\right)^M \\
&\approx \left(1 - \frac{1}{\Gamma_{\text{RD}}} e^{-\frac{\Gamma_T}{\Gamma_{\text{RD}}}} e^{-\frac{\Gamma_T}{\Gamma_{\text{SR}}}} \left(\Gamma_{\text{RD}} \xi K_1(\xi) - \frac{4\Gamma_T \Gamma_{\text{RR}}}{\Gamma_{\text{SR}}} K_0(\xi)\right)\right)^M \qquad (4.40)
\end{aligned}$$

where $K_n(x) = \int_0^{\infty} e^{-x\cosh(t)} \cosh(nt) dt$ is the n^{th} order modified Bessel function of the second kind, $\xi = 2\sqrt{\frac{\Gamma_T(1+\Gamma_T)}{\Gamma_{\text{SR}}\Gamma_{\text{RD}}}}$ and using small approximations of $K_1(\xi)$ and $K_0(\xi) \cong -\eta - \log\frac{\xi}{2}$, $\eta = \frac{1}{\Gamma_{\text{RD}}}$, we get,

$$\Pr\left(\gamma_{\text{MMSE-DFE}} \leq \Gamma_T\right) \leq \left(1 - e^{-\frac{\Gamma_T}{\Gamma_{\text{RD}}}} e^{-\frac{\Gamma_T}{\Gamma_{\text{SR}}}} \left(1 - \frac{4\Gamma_T \Gamma_{\text{RR}}}{\Gamma_{\text{SR}}\Gamma_{\text{RD}}}(-\eta - \log(\frac{\xi}{2}))\right)\right)^M \qquad (4.41)$$

The outage probability degradation due to the RSI, now decreases as Γ_{RD} grows and thus, under moderate RSI, we can expect that the equalization at D leads to more graceful performance degradation compared to treating RSI as noise.

The second case is where RSI is very strong, i.e., $\frac{\Gamma_{\text{SR}}\Gamma_{\text{RD}}}{2\Gamma_{\text{RR}}\Gamma_T} \ll 1$, we approximate $\frac{\Gamma_{\text{SR}} z}{\Gamma_{\text{SR}} z + 2\Gamma_T\Gamma_{\text{RR}}} \simeq \frac{\Gamma_{\text{SR}} z}{2\Gamma_T\Gamma_{\text{RR}}}$. Using this in (4.39), we have,

$$\begin{aligned}
\Pr\left(\gamma_{\text{MMSE-DFE}} \leq \Gamma_T\right) &\leq \left(1 - \frac{\xi^2 K_2(\xi) \Gamma_{\text{SR}}\Gamma_{\text{RD}} e^{-\frac{\Gamma_T}{\Gamma_{\text{RD}}} - \frac{\Gamma_T}{\Gamma_{\text{SR}}}}}{4\Gamma_T\Gamma_{\text{RR}}}\right)^M \\
&\approx \left(1 - \frac{\Gamma_{\text{SR}}\Gamma_{\text{RD}} e^{-\frac{\Gamma_T}{\Gamma_{\text{RD}}} - \frac{\Gamma_T}{\Gamma_{\text{SR}}}}}{2\Gamma_T\Gamma_{\text{RR}}}\right)^M \qquad (4.42)
\end{aligned}$$

where we approximate $K_2(\xi) \approx 2\xi^{-2}$. Since $\frac{\Gamma_{\text{SR}}\Gamma_{\text{RD}}}{2\Gamma_{\text{RR}}\Gamma_T} \ll 1$, we can observe that the outage probability here remains close to one, which is understandable as, under strong RSI, the relay wastes most of its transmit power to amplify the RSI.

4.5 SIMULATION RESULTS

In this section, we present the outage performance of full-duplex amplify-and-forward MIMO relaying system with different combining techniques at the relay, based on the output SNR of the equalizers at the destination. We also present the results for outage probability comparison of EGT and AS for different M values. For the case of antenna selection, we present the results for a bound on the outage probability and we also discuss the effects of the number of antennas at the relay R on the outage probability. All the simulations presented are performed with the assumption that the destination employs an MMSE-DFE equalizer.

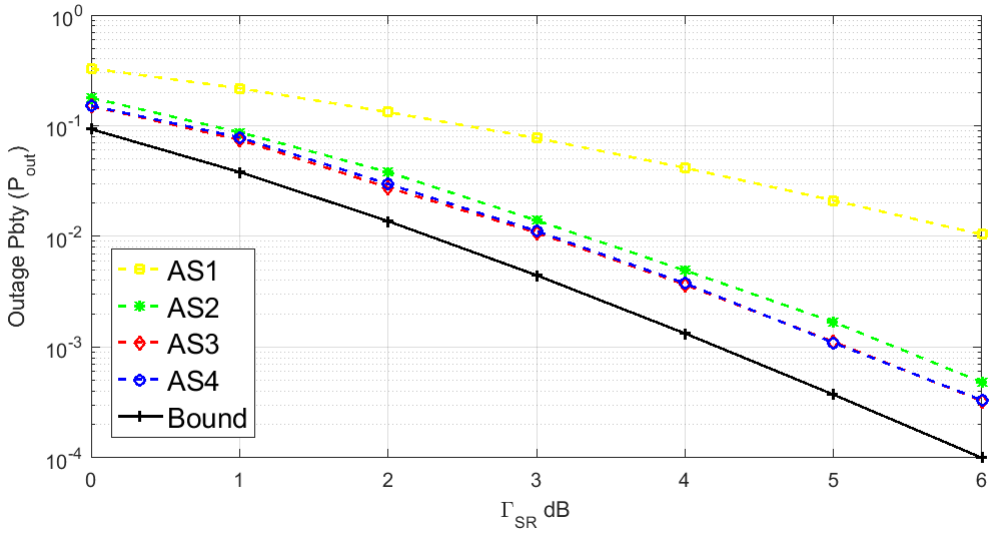

Figure 4.3: Outage Probability Comparison of AS1, AS2, AS3, AS4 for a system with 8×8 FD AF MIMO Relay with fixed RSI power, where destination employs MMSE-DFE equalizer and $\Gamma_{\mathrm{RD}} = 15$ dB, $\Gamma_{\mathrm{RR}} = 5$ dB,$R_T = 1$ bps/Hz

Fig. 4.3 shows the outage performance of different antenna selection criteria discussed in the previous section. We can observe that using the AS4 technique, this system with $M = 8$ can achieve a probability of 10^{-3} for an outage, when the aver-

age SNR Γ_{SR} is approximately about 5 dB. Also, it is evident from the figure, that AS1 performs poorly among all the selection criteria and AS2, AS3 and AS4 provide almost the same performance. One can prefer AS3 over AS2 because of the fact that, AS3 does not require any knowledge of the RSI channel. One can choose to apply any among AS2, AS3, AS4 criteria, but due to the equalizer present at D, AS4 might require more computation than AS2 and AS3. It can be noted that the bound derived on antenna selection scheme with MMSE-DFE equalizer at the destination, serves as a tight bound.

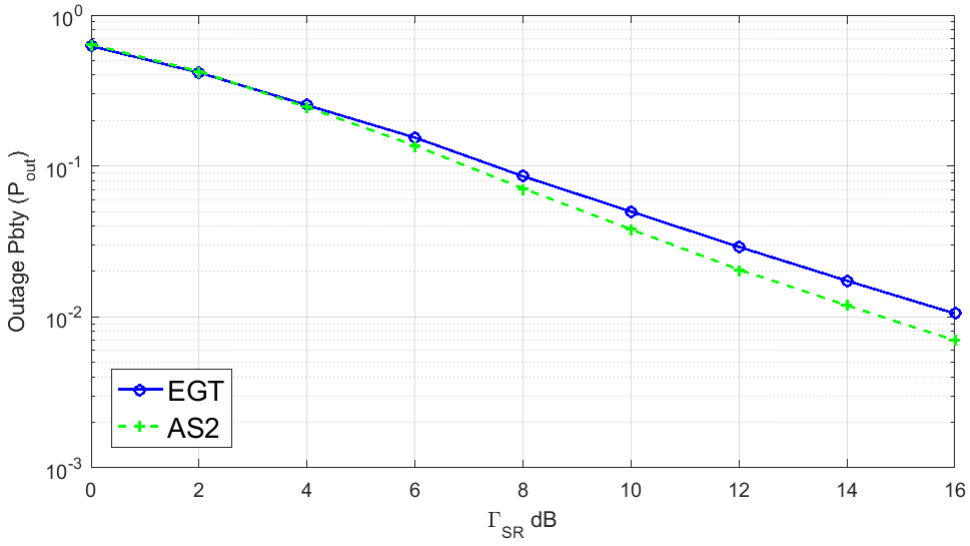

Figure 4.4: Outage Probability Comparison of EGT, AS2 for a system with 2×2 FD AF MIMO Relay with fixed RSI power, where destination employs MMSE-DFE equalizer and $\Gamma_{\mathrm{RD}} = 15$ dB, $\Gamma_{\mathrm{RR}} = 5$ dB,$R_T = 1$ bps/Hz

Fig. 4.4 shows the comparison of the two schemes EGT and AS2 for a fixed RSI power. The full-duplex relay in the system is assumed to have 2 transmit-receive antenna pairs i.e., $M = 2$ and the RSI is assumed to be non-variant. In such a scenario, we can observe from the figure, that at a low SNR regime, until a particular

value, EGT performs better than AS2. At approximately a value of 4 dB for Γ_{SR}, we can notice that AS2 cross overs EGT and outperforms it as the SNR grows high.

Fig. 4.5 shows the similar comparison to that of Fig. 4.4, but for a varying RSI power. Here the RSI at the relay is considered to be variant with M being 2. It can be clearly observed that, though EGT performs better than AS2 for low SNR values, AS2 outperforms EGT for high SNR as in the fixed RSI case, except that the crossover point moved to the right, i.e., where the crossover point is at 11 dB. Intuitively speaking, this can be explained by the fact that, in EGT, even though the

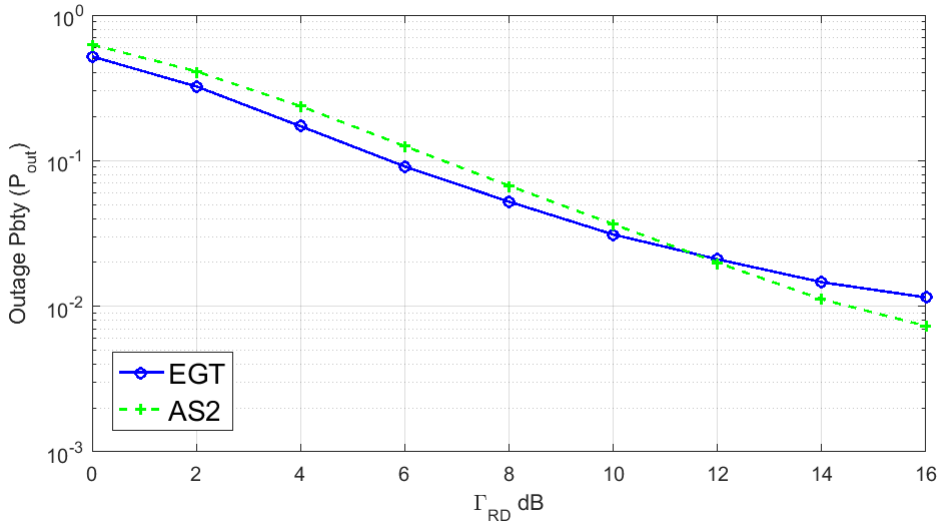

Figure 4.5: Outage Probability Comparison of EGT, AS2 for a system with 2×2 FD AF MIMO Relay with varying RSI power, where destination employs MMSE-DFE equalizer and $\Gamma_{\mathrm{SR}} = 15$ dB, $R_T = 1$ bps/Hz

total transmit power is equally shared among all transmit antennas, RSI is due to all the M transmit antennas. Whereas in AS (whatever may be the selection criterion), RSI is only due to one of the M transmit antennas that is active. This can give rise to the thought that, as SNR increases, the effect of RSI in AS diminishes faster than that of EGT.

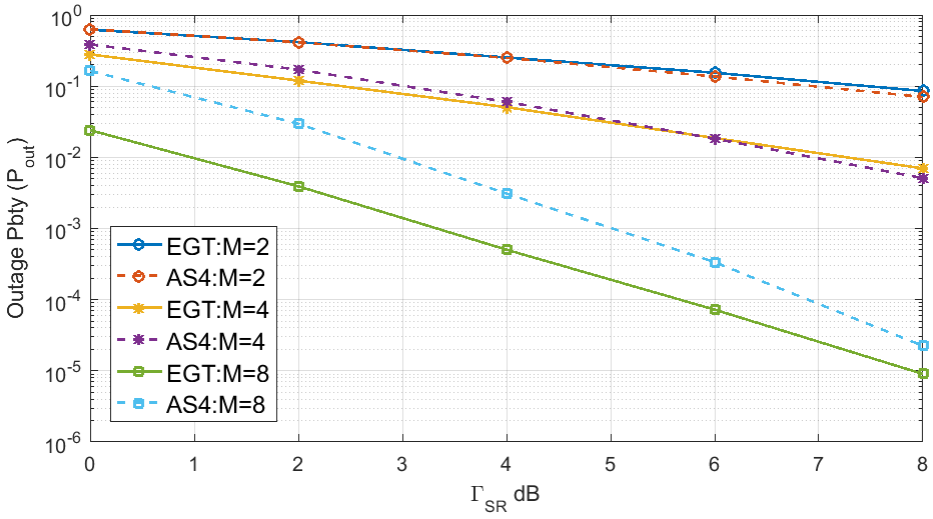

Figure 4.6: Outage Probability Comparison of EGT and AS4 for a system with $2 \times 2, 4 \times 4, 8 \times 8$ FD AF MIMO Relays with fixed RSI power, where destination employs MMSE-DFE equalizer and $\Gamma_{\mathrm{RD}} = 15$ dB, $\Gamma_{\mathrm{RR}} = 5$ dB,$R_T = 1$ bps/Hz

Fig. 4.6 shows the outage performance analysis for different M values at relay with fixed RSI power. We can observe that an outage probability of about 10^{-5} can be achieved with just an SNR of 8 dB when we have an 8×8 relay. Also, it is to be noted that, as M increases, the crossover point between EGT and AS slides further to the right. This can be again understood from the fact stated above, as the M value goes high, the diversity increases and the accordingly, RSI corresponds to M antennas in EGT and one antenna in AS.

Fig .4.7 presents an outage comparison between the EGT and all the selection criteria in AS technique. From (4.4), it is clear that as the rate of transmission R_T increases, the threshold Γ_T for the outage increases and hence the probability of outage increases. If the system is designed to maintain an outage probability of less than 10^{-2}, from the figure, it is evident that the target rate should not exceed 1 bps/Hz. Also, one can notice that EGT and AS schemes in this simulation have

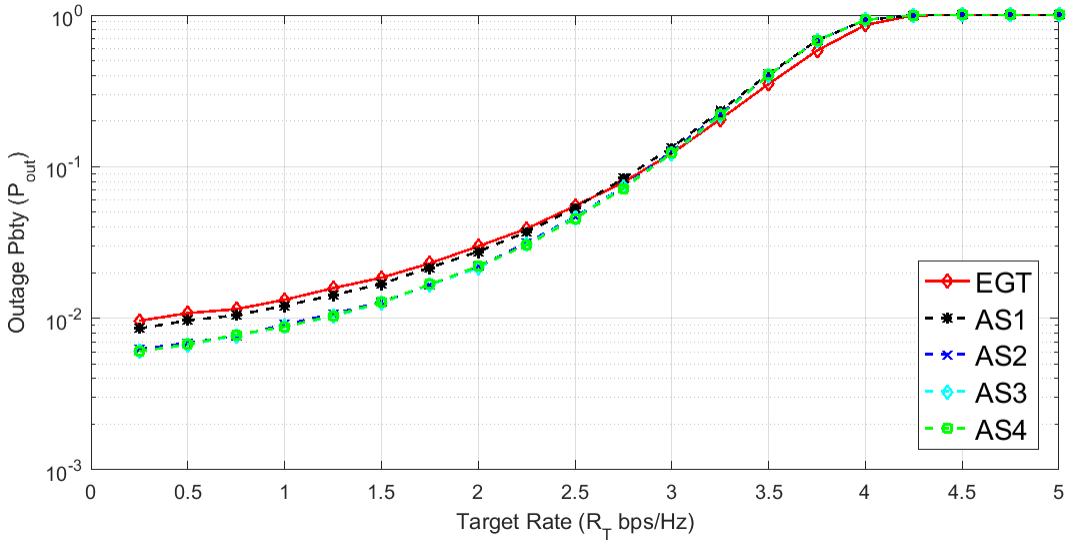

Figure 4.7: Outage Probability vs Target Rate (R_T) comparison of EGT and AS selection criteria for a system with 2×2 FD AF MIMO Relay with fixed RSI power, where destination employs MMSE-DFE equalizer and $\Gamma_{\mathrm{SR}} = \Gamma_{\mathrm{RD}} = 15$ dB, $\Gamma_{\mathrm{RR}} = 5$ dB

a crossover point at a target rate of 3 bps/Hz, which indicates that for a given SNR value, antenna selection technique performs better than EGT up to a transmission rate of 3 bps/ Hz.

4.6 SUMMARY

In this chapter, assuming equalization at the destination, we proposed equal-gain transmission and antenna selection techniques, that can compensate the effect of RSI to a considerable extent. With EGT, we derived the overall system transfer function and thus, the power spectral densities with respect to both the source and the noise which can be used to compute the output SNR at the destination. With AS, we discussed different selection criteria to select the transmit-receive antenna pair and the corresponding power spectral densities with respect to source and noise are computed.

Additionally, we derived a lower bound on the outage probability of antenna selection and found that to be the tightest bound possible. The outage performances for both EGT and different AS schemes are analyzed. In the simulation results, we have shown that the proposed schemes crossover at a particular point depending on the number of transmitting antennas at the relay and after the cross-over point AS outperforms EGT, due to the fact of reduced RSI in AS when compared to EGT.

Chapter 5

CONCLUSIONS AND FUTURE WORKS

In this chapter, we present the conclusions that can be drawn from this thesis and then, we proceed further to discuss the scope of further research in areas related to full-duplex relaying networks.

5.1 CONCLUSIONS

In chapters 1,2, we discussed and established a detailed understanding of the basics of co-operative communications, full-duplex relaying, self-interference cancellation techniques, benefits of MIMO and different diversity combining techniques in practice. These concepts helped in designing the system model that is in consideration for the rest of the thesis.

In Chapter 3, we discussed a couple of methods to derive the input-output relationship of a two-hop full-duplex amplify-and-forward MIMO relay network in the Z-transform domain. One of the methods use the signal flow graph approach and gives the closed form transfer function using Mason's gain formula. Although this technique is very efficient than the traditional recursive substitution methods, and provide us with the knowledge about the degree of the polynomials involved in the effective channel of the system in a easy manner, as the number of antennas at the relay increase or the number of relays in between the source and destination increase, considering the residual self-interference at each relay and the inter-relay interference in respective cases, this approach seems to turn out much complex than what it is. Hence, we came up with a simple linear algebraic approach, that gives the end-to-end effective channel equations with respect to the signal and noise inputs very easily for

any number of antennas at the relay. This technique can be modified accordingly and can be made applicable for any number of relays in between source and destination.

In Chapter 4, we presented different equalization techniques at the destination and their output SNRs are discussed. Assuming one of the equalization techniques at the destination, we proposed two different transmit combining techniques to be implemented at the relay. One of them is the equal-gain transmission, where the total transmit power at the relay is equally shared among all the transmit antennas and pre-coding is performed to achieve diversity and enhanced SNR at destination by phase cancellation. Whereas in the other approach i.e., in Antenna Selection, we choose only transmit-receive antenna pair among all at the relay based on different selection criteria and at any point of time, the selected antenna pair will be active. The total transmit power at the relay in this case, is allocated to the only antenna that is transmitting. The computation of the amplification factors and the effective channels for each of the schemes are presented. Their outage performances are analyzed and compared. For the case of antenna selection, a lower bound for the outage probability is derived assuming the presence of MMSE-DFE equalizer at the destination. We have shown the simulation results that quantitatively compare the proposed techniques.

5.2 FUTURE WORKS

Now, a few ideas that can help modify the proposed approaches and make them applicable to more generalized scenarios or system models are discussed briefly.

MRC and MRT at Relay

As we are already aware that MRC gives us the optimal performance among different existing receive combining techniques and after analyzing the performance of the EGT and antenna selection techniques, it is time to think and analyze the performance for

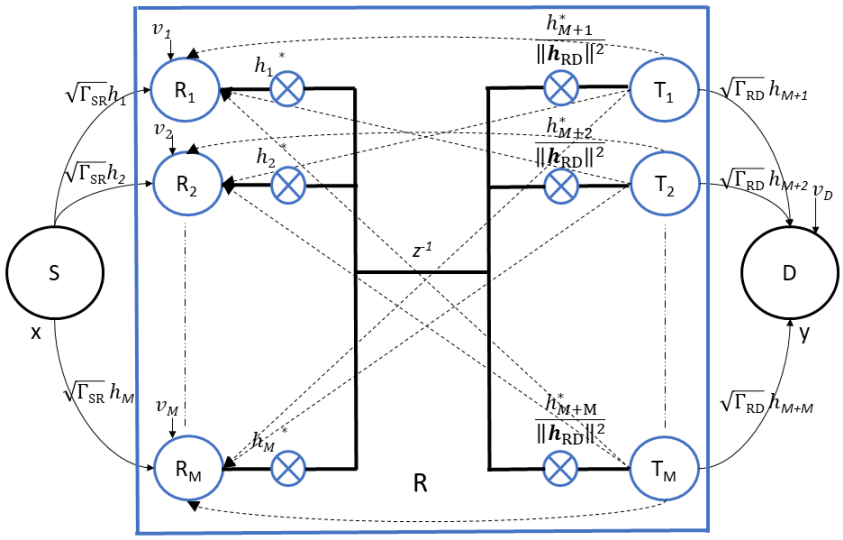

Figure 5.1: Block Diagram for a system with MRC and MRT at FD AF MIMO Relay

combination of MRC and MRT at relay. In EGT, we have seen that it is sufficient to have the knowledge of phase information of the channels and the total transmit power is shared equally among all the transmit antennas, irrespective of the channel strength. By doing this, the strongest and the weakest of the channels share same power which might not give the best performance possible. Whereas by using maximal ratio transmission (MRT), which requires the knowledge of both amplitude and phase information of the channels, we can get to know the channel strengths and the total transmit power can be dynamically allocated to transmit antennas depending on the strength of the corresponding channels. One can focus on this power optimization problem, so that it is not too complex for the implementation. It can be understood from Fig. 5.1 that one can implement MRC on the receive side of the relay, amplify the scalar output of MRC combiner by implementing MRT at the transmit side of the relay before forwarding it to the destination.

For such implementation, the relay's received signal can be given as:

$$\mathbf{r}(z) = \sqrt{\Gamma_{\mathrm{SR}}}\mathbf{h}_{\mathrm{SR}}x(z) + \sqrt{\Gamma_{\mathrm{RR}}}\mathbf{H}\mathbf{t}(z) + \mathbf{v}(z) \tag{5.1}$$

On implementing MRC over the received signals at relay, the resultant scalar output of the combiner is given as:

$$\begin{aligned} r_{\mathrm{MRC}}(z) &= \mathbf{h}_{\mathrm{SR}}^{\mathsf{H}}\mathbf{r}(z) \\ &= \sqrt{\Gamma_{\mathrm{SR}}}\|\mathbf{h}_{\mathrm{SR}}\|^2 x(z) + \sqrt{\Gamma_{\mathrm{RR}}}\mathbf{h}_{\mathrm{SR}}^{\mathsf{H}}\mathbf{H}\mathbf{t}(z) + \mathbf{h}_{\mathrm{SR}}^{\mathsf{H}}\mathbf{v}(z) \end{aligned} \tag{5.2}$$

where $\mathbf{h}_{\mathrm{SR}}^{\mathsf{H}}$ denotes the conjugate transpose of the vector $\mathbf{h}_{\mathrm{SR}}$.

The amplification factor $\mathbf{g}$ is given by

$$\mathbf{g} = \begin{bmatrix} g_{M+1} & g_{M+2} & \cdots & g_{M+M} \end{bmatrix}^{\mathsf{T}} = \frac{\mathbf{h}_{\mathrm{RD}}^{*}}{\|\mathbf{h}_{\mathrm{RD}}\|^2} \tag{5.3}$$

where $\mathbf{h}_{\mathrm{RD}}^{*}$ denotes the element wise conjugate of the vector $\mathbf{h}_{\mathrm{RD}}$.

At relay, after amplifying using MRT, the transmit signal is given as:

$$\begin{aligned} \mathbf{t}(z) &= \mathbf{g}r_{\mathrm{MRC}}(z)z^{-1} \\ &= \sqrt{\Gamma_{\mathrm{SR}}}\frac{\|\mathbf{h}_{\mathrm{SR}}\|^2}{\|\mathbf{h}_{\mathrm{RD}}\|^2}\mathbf{h}_{\mathrm{RD}}^{*}x(z)z^{-1} + \frac{\sqrt{\Gamma_{\mathrm{RR}}}}{\|\mathbf{h}_{\mathrm{RD}}\|^2}\mathbf{h}_{\mathrm{RD}}^{*}\mathbf{h}_{\mathrm{SR}}^{\mathsf{H}}\mathbf{H}\mathbf{t}(z)z^{-1} \\ &\qquad + \frac{1}{\|\mathbf{h}_{\mathrm{RD}}\|^2}\mathbf{h}_{\mathrm{RD}}^{*}\mathbf{h}_{\mathrm{SR}}^{\mathsf{H}}\mathbf{v}(z)z^{-1} \end{aligned} \tag{5.4}$$

The received signal at D is again same as in 3.22. The power spectral densities with respect to signal from the source and noise at the relay can be computed the same way as we did for EGT and are given as :

$$S_s(f) = \left| \sqrt{\Gamma_{\mathrm{SR}}\Gamma_{\mathrm{RD}}}\mathbf{h}_{\mathrm{SR}}^{\mathsf{H}} \left(\mathbf{I}e^{j2\pi f} - \frac{\sqrt{\Gamma_{\mathrm{RR}}}}{\|\mathbf{h}_{\mathrm{RD}}\|^2}\mathbf{H}\mathbf{h}_{\mathrm{RD}}^{*}\mathbf{h}_{\mathrm{SR}}^{\mathsf{H}} \right)^{-1} \mathbf{h}_{\mathrm{SR}} \right|^2 \tag{5.5}$$

$$S_\nu(f) = 1 + \left\| \sqrt{\Gamma_{\mathrm{RD}}}\mathbf{h}_{\mathrm{SR}}^{\mathsf{H}} \left(\mathbf{I}e^{j2\pi f} - \frac{\sqrt{\Gamma_{\mathrm{RR}}}}{\|\mathbf{h}_{\mathrm{RD}}\|^2}\mathbf{H}\mathbf{h}_{\mathrm{RD}}^{*}\mathbf{h}_{\mathrm{SR}}^{\mathsf{H}} \right)^{-1} \right\|^2 \tag{5.6}$$

Antenna Selection with M^2 possible selections:

In the AS strategy discussed in chapter 4, from Fig. 4.2, we can see that there are M transmit-receive antenna pairs and one among M is chosen to be active. If we slightly modify the relay, we can think of M^2 possible transmit-receive antenna pairs and choose one among them to transmit. As we provide with more pairs, there is definitely a possibility of enhancing the performance with the same selection criteria used in this thesis. This can be understood clearly from Fig. 5.2, which is a simple example with 2×2 relay. Earlier, there are only 2 pairs of antennas which are $\mathrm{R}_1 - \mathrm{T}_1$

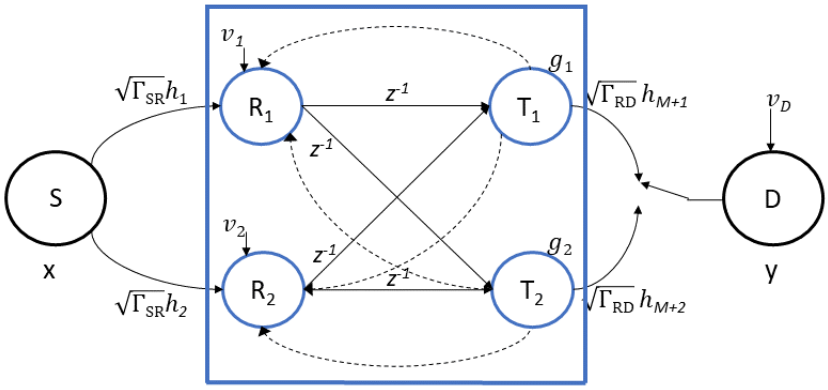

Figure 5.2: Block Diagram for a system with modified AS at FD AF 2×2 Relay

and $\mathrm{R}_2 - \mathrm{T}_2$. Whereas now, we consider 4 possible pairs $\mathrm{R}_1 - \mathrm{T}_1$, $\mathrm{R}_1 - \mathrm{T}_2$, $\mathrm{R}_2 - \mathrm{T}_1$ and $\mathrm{R}_2 - \mathrm{T}_2$. Similarly, for a relay with M transmit and receive antennas we can find M^2 possible pairs to choose one particular pair to be active. Any of the four different selection criteria discussed in chapter 4 can be applied to this case and one among M^2 antenna pairs can be chosen and RSI is due to only one transmit antenna. The received signal at relay is given by:

$$r_i[n] = \sqrt{\Gamma_{\mathrm{SR}}} h_i x[n] + \sqrt{\Gamma_{\mathrm{RR}}} h_{ji} t_j[n] + \nu_i[n] \tag{5.7}$$

The transmit signal can be written as:

$$t_j[n] = g_j r_i[n-1] \tag{5.8}$$

The signal received at D is:

$$\begin{aligned} y[n] &= \sqrt{\Gamma_{\mathrm{RD}}} h_{M+j} t_j[n] + \nu_D[n] \\ &= \sqrt{\Gamma_{\mathrm{SR}}\Gamma_{\mathrm{RD}}} h_i h_{M+j} g_j x[n-1] + \sqrt{\Gamma_{\mathrm{RR}}\Gamma_{\mathrm{RD}}} h_{ji} h_{M+j} g_j t_j[n-1] \\ &\quad + \sqrt{\Gamma_{\mathrm{RD}}} h_{M+j} g_j \nu_i[n] + \nu_D[n] \end{aligned} \tag{5.9}$$

The power spectral densities with respect to signal from source and noise at relay

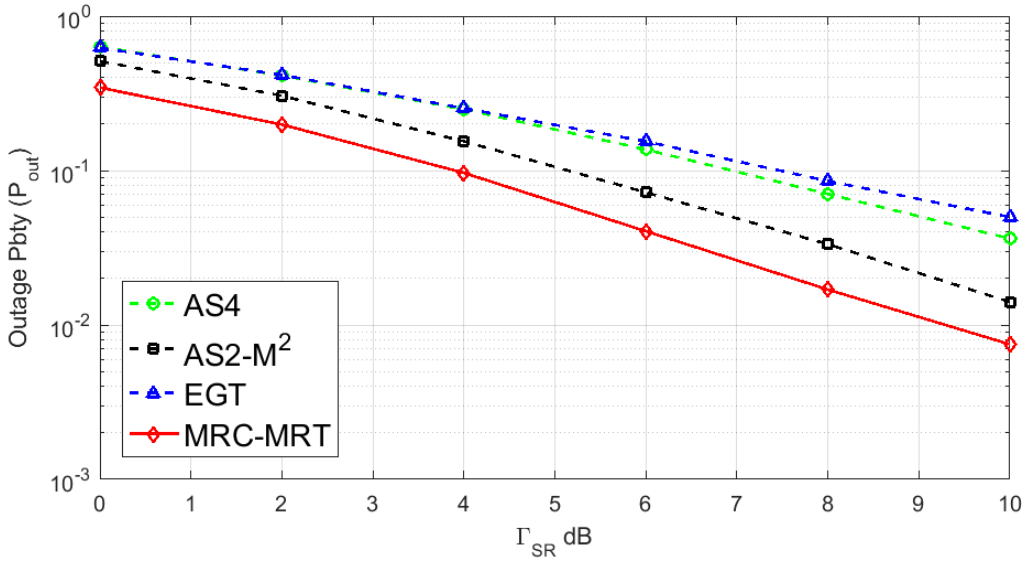

Figure 5.3: Outage Probability Comparison of AS4, EGT, AS2-M^2 selections and MRC-MRT for M=2 with fixed RSI power, where destination employs MMSE-DFE equalizer and $\Gamma_{\mathrm{RD}} = 15$ dB, $\Gamma_{\mathrm{RR}} = 5$ dB,$R_T = 1$ bps/Hz

can be computed same way as we did in AS techniques discussed in chapter 4 and are given by:

$$S_s(f) = \left| \sqrt{\Gamma_{\mathrm{SR}}\Gamma_{\mathrm{RD}}} h_i h_{M+j} g_j \left(e^{j2\pi f} - \sqrt{\Gamma_{\mathrm{RR}}} h_{ji} g_j \right)^{-1} \right|^2 \tag{5.10}$$

$$S_\nu(f) = 1 + \left| \sqrt{\Gamma_{\mathrm{RD}}} h_{M+j} g_j \left(e^{j2\pi f} - \sqrt{\Gamma_{\mathrm{RR}}} h_{ji} g_j \right)^{-1} \right|^2 \tag{5.11}$$

With the expressions, we have given for MRC-MRT and AS with M^2 possible selections, we have performed simple simulations to compare their performances with the EGT and AS schemes discussed in chapter 4. Fig. 5.3 evidently proves our point that MRC-MRT outperforms all the other techniques used in this thesis but at the cost of increased complexity. We can observe that there is around 3 dB gap between the MRC-MRT and EGT. AS2 with M^2 possible selections although is not as good as MRC-MRT, it performs better than the previously discussed AS schemes and EGT as expected.

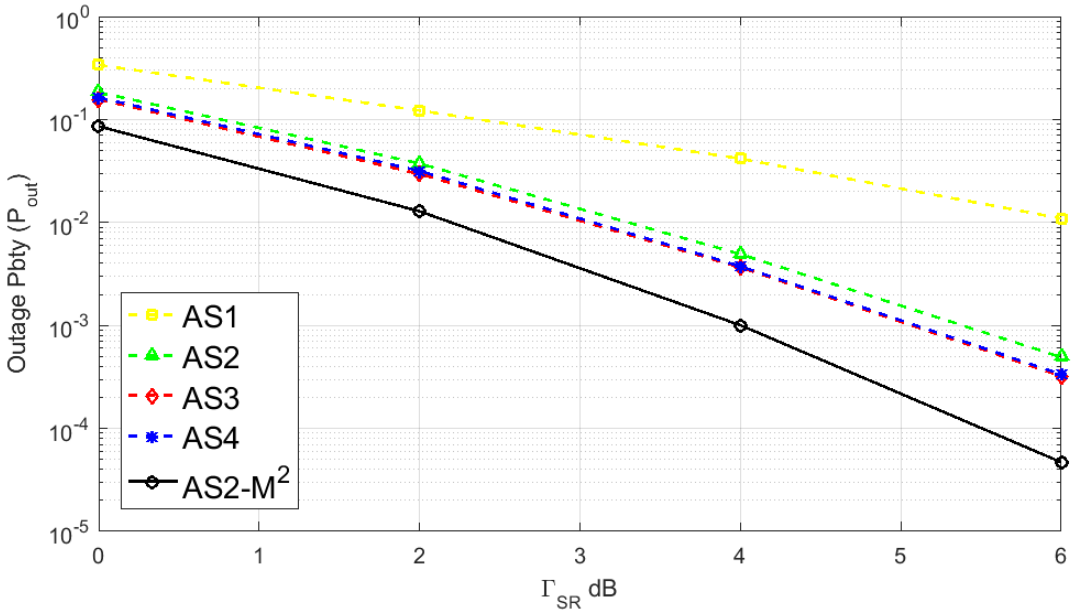

Figure 5.4: Outage Probability comparison of AS-1,2,3,4 and AS2-M^2 selections for M=8 with fixed RSI power, where destination employs MMSE-DFE equalizer and $\Gamma_{\mathrm{RD}} = 15$ dB, $\Gamma_{\mathrm{RR}} = 5$ dB,$R_T = 1$ bps/Hz

From Fig. 5.4, we can clearly observe that for any system with a given target rate of transmission and fixed RSI power, AS with M^2 possible antenna pairs performs

better than the AS with M possible antenna pairs discussed in chapter 4. This can be clearly understood from the ordered statistics involved in both the scenarios. It can be observed that there is almost 1 dB gap between AS4 and AS2-M^2 curves.

The analysis in this thesis is presented by considering a system that is comprised of a source and a destination with a single antenna and a relay with multiple transmit and receive antennas. This can be extended to systems with source and destination having multiple antennas and to even more generalized systems with multiple MIMO relays cascaded in series or parallel. One can even think of Multi-User MIMO implementations with these, where the system can have multiple source and destination nodes connected by the MIMO relay.

REFERENCES

[1] A. Goldsmith, *Wireless communications*. Cambridge university press, 2005.

[2] M. Nakagami, "The m-distributiona general formula of intensity distribution of rapid fading," in *Statistical methods in radio wave propagation*. Elsevier, 1960, pp. 3–36.

[3] S. AlMaeeni, P. C. Sofotasios, S. Muhaidat, and G. K. Karagiannidis, "Analysis of differentially modulated cooperative communications over asymmetric fading channels," in *Advanced Communication Technologies and Networking (CommNet), 2018 International Conference on*. IEEE, 2018, pp. 1–8.

[4] P. Gupta and P. Kumar, "Towards an information theory of large networks: An achievable rate region," *IEEE Transactions on Information Theory*, vol. 49, no. 8, pp. 1877–1894, 2003.

[5] L.-L. Xie and P. R. Kumar, "An achievable rate for the multiple-level relay channel," *IEEE Transactions on Information Theory*, vol. 51, no. 4, pp. 1348–1358, 2005.

[6] G. Kramer, M. Gastpar, and P. Gupta, "Cooperative strategies and capacity theorems for relay networks," 2004.

[7] H. Bolcskei, R. U. Nabar, O. Oyman, and A. J. Paulraj, "Capacity scaling laws in mimo relay networks," *IEEE Transactions on Wireless Communications*, vol. 5, no. 6, pp. 1433–1444, 2006.

[8] M. O. Hasna and M.-S. Alouini, "End-to-end performance of transmission systems with relays over rayleigh-fading channels," *IEEE transactions on Wireless Communications*, vol. 2, no. 6, pp. 1126–1131, 2003.

[9] C. Jeong, H.-M. Kim, H.-K. Song, and I.-M. Kim, "Relay precoding for nonregenerative mimo relay systems with partial csi in the presence of interferers," *IEEE Transactions on Wireless Communications*, vol. 11, no. 4, pp. 1521–1531, 2012.

[10] R. Pabst, B. H. Walke, D. C. Schultz, P. Herhold, H. Yanikomeroglu, S. Mukherjee, H. Viswanathan, M. Lott, W. Zirwas, M. Dohler *et al.*, "Relay-based deployment concepts for wireless and mobile broadband radio," *IEEE Communications Magazine*, vol. 42, no. 9, pp. 80–89, 2004.

[11] J. N. Laneman, D. N. Tse, and G. W. Wornell, "Cooperative diversity in wireless networks: Efficient protocols and outage behavior," *IEEE Transactions on Information theory*, vol. 50, no. 12, pp. 3062–3080, 2004.

[12] R. U. Nabar, H. Bolcskei, and F. W. Kneubuhler, "Fading relay channels: Performance limits and space-time signal design," *IEEE Journal on Selected Areas in communications*, vol. 22, no. 6, pp. 1099–1109, 2004.

[13] X. J. Zhang and Y. Gong, "Adaptive power allocation for regenerative relaying with multiple antennas at the destination," *IEEE Transactions on Wireless Communications*, vol. 8, no. 6, 2009.

[14] J. Kaleva, A. Tolli, and M. Juntti, "User admission for multi-user regenerative relay mimo systems," in *Communications (ICC), 2013 IEEE International Conference on*. IEEE, 2013, pp. 5850–5854.

[15] G. Levin and S. Loyka, "Amplify-and-forward versus decode-and-forward relaying: which is better?" in *22th International Zurich Seminar on Communications (IZS)*. Eidgenössische Technische Hochschule Zürich, 2012.

[16] J. Boyer, D. D. Falconer, and H. Yanikomeroglu, "Multihop diversity in wireless relaying channels," *IEEE Transactions on communications*, vol. 52, no. 10, pp. 1820–1830, 2004.

[17] G. Farhadi and N. C. Beaulieu, "On the ergodic capacity of multi-hop wireless relaying systems," *IEEE Transactions on Wireless Communications*, vol. 8, no. 5, 2009.

[18] Y. Fan and J. Thompson, "Mimo configurations for relay channels: Theory and practice," *IEEE Transactions on Wireless Communications*, vol. 6, no. 5, 2007.

[19] S. Loyka and G. Levin, "On outage probability and diversity-multiplexing tradeoff in mimo relay channels," *IEEE Transactions on Communications*, vol. 59, no. 6, pp. 1731–1741, 2011.

[20] A. Otyakmaz, R. Schoenen, S. Dreier, and B. H. Walke, "Parallel operation of half-and full-duplex fdd in future multi-hop mobile radio networks," in *Wireless Conference, 2008. EW 2008. 14th European*. IEEE, 2008, pp. 1–7.

[21] T. Riihonen, S. Werner, and R. Wichman, "Comparison of full-duplex and half-duplex modes with a fixed amplify-and-forward relay," in *Wireless communications and networking conference, 2009. WCNC 2009. IEEE*. IEEE, 2009, pp. 1–5.

[22] D. Soldani and S. Dixit, "Wireless relays for broadband access [radio communications series]," *IEEE communications Magazine*, vol. 46, no. 3, 2008.

[23] A. Sabharwal, P. Schniter, D. Guo, D. W. Bliss, S. Rangarajan, and R. Wichman, "In-band full-duplex wireless: Challenges and opportunities," *IEEE Journal on selected areas in communications*, vol. 32, no. 9, pp. 1637–1652, 2014.

[24] D. Kim, H. Lee, and D. Hong, "A survey of in-band full-duplex transmission: From the perspective of phy and mac layers," *IEEE Communications Surveys & Tutorials*, vol. 17, no. 4, pp. 2017–2046, 2015.

[25] S. Hong, J. Brand, J. Choi, M. Jain, J. Mehlman, S. Katti, and P. Levis, "Applications of self-interference cancellation in 5g and beyond," *IEEE Communications Magazine*, vol. 52, no. 2, pp. 114–121, 2014.

[26] C. Li, X. Wang, L. Yang, and W.-P. Zhu, "A joint source and relay power allocation scheme for a class of mimo relay systems," *IEEE Transactions on Signal Processing*, vol. 57, no. 12, pp. 4852–4860, 2009.

[27] H. Ju, E. Oh, and D. Hong, "Improving efficiency of resource usage in two-hop full duplex relay systems based on resource sharing and interference cancellation," *IEEE Transactions on Wireless Communications*, vol. 8, no. 8, 2009.

[28] P. Lioliou, M. Viberg, M. Coldrey, and F. Athley, "Self-interference suppression in full-duplex mimo relays," in *Signals, Systems and Computers (ASILOMAR), 2010 Conference Record of the Forty Fourth Asilomar Conference on.* IEEE, 2010, pp. 658–662.

[29] T. Riihonen, A. Balakrishnan, K. Haneda, S. Wyne, S. Werner, and R. Wichman, "Optimal eigenbeamforming for suppressing self-interference in full-duplex mimo relays," in *Information Sciences and Systems (CISS), 2011 45th Annual Conference on.* IEEE, 2011, pp. 1–6.

[30] T. Riihonen, S. Werner, and R. Wichman, "Residual self-interference in full-duplex mimo relays after null-space projection and cancellation," in *Signals, Systems and Computers (ASILOMAR), 2010 Conference Record of the Forty Fourth Asilomar Conference on.* IEEE, 2010, pp. 653–657.

[31] B. P. Day, A. R. Margetts, D. W. Bliss, and P. Schniter, "Full-duplex mimo relaying: Achievable rates under limited dynamic range," *IEEE Journal on Selected Areas in Communications*, vol. 30, no. 8, pp. 1541–1553, 2012.

[32] I. Krikidis, H. A. Suraweera, P. J. Smith, and C. Yuen, "Full-duplex relay selection for amplify-and-forward cooperative networks," *IEEE Transactions on Wireless Communications*, vol. 11, no. 12, pp. 4381–4393, 2012.

[33] K. Yang, H. Cui, L. Song, and Y. Li, "Efficient full-duplex relaying with joint antenna-relay selection and self-interference suppression," *IEEE Transactions on Wireless Communications*, vol. 14, no. 7, pp. 3991–4005, 2015.

[34] M. Toka and O. Kucur, "Outage performance of dual hop full-duplex mimo relay networks with tas/mrc over rayleigh fading channels," in *Wireless Communication Systems (ISWCS), 2016 International Symposium on.* IEEE, 2016, pp. 99–103.

[35] S. Han, I. Chih-Lin, Z. Xu, C. Pan, and Z. Pan, "Full duplex: Coming into reality in 2020?" in *Global Communications Conference (GLOBECOM), 2014 IEEE.* IEEE, 2014, pp. 4776–4781.

[36] N. H. Mahmood, G. Berardinelli, F. M. Tavares, and P. Mogensen, "On the potential of full duplex communication in 5g small cell networks," in *Vehicular Technology Conference (VTC Spring), 2015 IEEE 81st.* IEEE, 2015, pp. 1–5.

[37] Z. Zhang, X. Chai, K. Long, A. V. Vasilakos, and L. Hanzo, "Full duplex techniques for 5g networks: self-interference cancellation, protocol design, and relay selection," *IEEE Communications Magazine*, vol. 53, no. 5, pp. 128–137, 2015.

[38] W. Cheng, X. Zhang, and H. Zhang, "Heterogeneous statistical qos provisioning over 5g wireless full-duplex networks," in *Computer Communications (INFOCOM), 2015 IEEE Conference on*. IEEE, 2015, pp. 55–63.

[39] T. M. Kim and A. Paulraj, "Outage probability of amplify-and-forward cooperation with full duplex relay," in *Wireless Communications and Networking Conference (WCNC), 2012 IEEE*. IEEE, 2012, pp. 75–79.

[40] A. Sureshbabu, *Outage Probability of Multi-hop Networks with Amplify-and-Forward Full-duplex Relaying*. Arizona State University, 2016.

[41] S.-H. Tsai, "An equal gain transmission in mimo wireless communications," in *Global Telecommunications Conference (GLOBECOM 2010), 2010 IEEE*. IEEE, 2010, pp. 1–5.

[42] T. M. Kim, A. Ghaderipoor, and A. Paulraj, "Antenna selection and power combining for transmit beamforming in mimo systems," in *Global Communications Conference (GLOBECOM), 2012 IEEE*. IEEE, 2012, pp. 4600–4605.

[43] Y. Deng, M. Elkashlan, P. L. Yeoh, N. Yang, and R. K. Mallik, "Cognitive mimo relay networks with generalized selection combining," *IEEE Transactions on Wireless Communications*, vol. 13, no. 9, pp. 4911–4922, 2014.

[44] Y. A. Al-Zahrani, N. K. Al-Mutairi, Y. Al-Hodhayf, and A. Al-Shahrani, "Performance of antenna selection for maximum ratio combining mimo system," in *Communication Software and Networks (ICCSN), 2011 IEEE 3rd International Conference on*. IEEE, 2011, pp. 642–645.

[45] N. Yang, P. L. Yeoh, M. Elkashlan, J. Yuan, and I. B. Collings, "Transmit antenna selection with maximal-ratio combining in mimo multiuser relay networks," in *Global Telecommunications Conference (GLOBECOM 2011), 2011 IEEE*. IEEE, 2011, pp. 1–5.

[46] Y. Deng, M. Elkashlan, P. L. Yeoh, T. Q. Duong, and R. K. Mallik, "Generalized selection combining in cognitive mimo relay networks," in *Communications (ICC), 2014 IEEE International Conference on*. IEEE, 2014, pp. 1472–1477.

[47] V. S. Krishna and M. R. Bhatnagar, "Performance analysis of sub-optimal transmit and receive antenna selection strategies in single relay based df cooperative mimo networks," in *Communications (NCC), 2014 Twentieth National Conference on*. IEEE, 2014, pp. 1–6.

[48] X. Li and C. Tepedelenlioglu, "Maximum likelihood channel estimation for residual self-interference cancellation in full duplex relays," in *Signals, Systems and Computers, 2015 49th Asilomar Conference on*. IEEE, 2015, pp. 807–811.

[49] X. Li, C. Tepedelenlioğlu, and H. Senol, "Optimal power allocation between training and data for mimo two-way relay channels," *IEEE Communications Letters*, vol. 19, no. 11, pp. 1941–1944, 2015.

[50] X. Li, C. Tepedelenlioğlu, and H. Şenol, "Channel estimation for residual self-interference in full-duplex amplify-and-forward two-way relays," *IEEE Transactions on Wireless Communications*, vol. 16, no. 8, pp. 4970–4983, 2017.

[51] X. Li, C. Tepedelenlioğlu, and H. Şenol, "Optimal training for residual self-interference in full duplex one-way relays," *submited to IEEE Transactions on Communications, http://arxiv.org/abs/1709.06140*.

[52] H. Şenol, X. Li, and C. Tepedelenlioğlu, "Rapidly time-varying channel estimation for full-duplex amplify-and-forward one-way relay networks," *IEEE Transactions on Signal Processing*, vol. 66, no. 11, pp. 3056–3069, 2018.

[53] S. Sandhu, R. Nabar, D. Gore, and A. Paulraj, "Introduction to space-time codes," *Applications of Space-Time Adaptive Processing, IEE Publishers http://www. stanford. edu/group/sarg/sandhu062503. pdf (Accessed on 18/07/2015)*, 2003.

[54] S. A. Ahson and M. Ilyas, *Get Certified: A Guide to Wireless Communication Engineering Technologies*. CRC Press, 2009.

[55] A. F. Molisch, *Wireless communications*. John Wiley & Sons, 2012, vol. 34.

[56] I. Rashid, "Mimo multi-hop relay systems," Ph.D. dissertation, University of Manchester, 2011.

[57] S. M. Alamouti, "A simple transmit diversity technique for wireless communications," *IEEE Journal on selected areas in communications*, vol. 16, no. 8, pp. 1451–1458, 1998.

[58] J. G. Proakis, "Digital communications. 1995," *McGraw-Hill, New York*.

[59] A. Mohammad, K. Sundaresan, S. Rangarajan, X. Zhang, and S. Barghi, "The case for antenna cancellation for scalable full-duplex wireless communications," *ACM Hotnets, Cambridge, MA, USA*, 2011.

[60] T. Riihonen, S. Werner, and R. Wichman, "Spatial loop interference suppression in full-duplex mimo relays," in *Signals, Systems and Computers, 2009 Conference Record of the Forty-Third Asilomar Conference on*. IEEE, 2009, pp. 1508–1512.

[61] T. Riihonen, S. Werner, R. Wichman, and E. Zacarias, "On the feasibility of full-duplex relaying in the presence of loop interference," in *Signal Processing Advances in Wireless Communications, 2009. SPAWC'09. IEEE 10th Workshop on*. IEEE, 2009, pp. 275–279.

[62] V. R. Cadambe and S. A. Jafar, "Degrees of freedom of wireless networks with relays, feedback, cooperation, and full duplex operation," *IEEE Transactions on Information Theory*, vol. 55, no. 5, pp. 2334–2344, 2009.

[63] M. Jain, J. I. Choi, T. Kim, D. Bharadia, S. Seth, K. Srinivasan, P. Levis, S. Katti, and P. Sinha, "Practical, real-time, full duplex wireless," in *Proceedings of the 17th annual international conference on Mobile computing and networking*. ACM, 2011, pp. 301–312.

[64] A. Host-Madsen and J. Zhang, "Capacity bounds and power allocation for wireless relay channels," *IEEE transactions on Information Theory*, vol. 51, no. 6, pp. 2020–2040, 2005.

[65] E. Everett, A. Sahai, and A. Sabharwal, "Passive self-interference suppression for full-duplex infrastructure nodes," *IEEE Transactions on Wireless Communications*, vol. 13, no. 2, pp. 680–694, 2014.

[66] E. Aryafar, M. A. Khojastepour, K. Sundaresan, S. Rangarajan, and M. Chiang, "Midu: Enabling mimo full duplex," in *Proceedings of the 18th annual international conference on Mobile computing and networking*. ACM, 2012, pp. 257–268.

[67] A. K. Khandani, "Methods for spatial multiplexing of wireless two-way channels," Oct. 19 2010, uS Patent 7,817,641.

[68] E. Everett, "Full-duplex infrastructure nodes: Achieving long range with half-duplex mobiles," Ph.D. dissertation, Rice University, 2012.

[69] J. I. Choi, M. Jain, K. Srinivasan, P. Levis, and S. Katti, "Achieving single channel, full duplex wireless communication," in *Proceedings of the sixteenth annual international conference on Mobile computing and networking*. ACM, 2010, pp. 1–12.

[70] E. Everett, M. Duarte, C. Dick, and A. Sabharwal, "Empowering full-duplex wireless communication by exploiting directional diversity," in *Signals, Systems and Computers (ASILOMAR), 2011 Conference Record of the Forty Fifth Asilomar Conference on*. IEEE, 2011, pp. 2002–2006.

[71] M. Duarte, C. Dick, and A. Sabharwal, "Experiment-driven characterization of full-duplex wireless systems," *IEEE Transactions on Wireless Communications*, vol. 11, no. 12, pp. 4296–4307, 2012.

[72] M. Duarte, A. Sabharwal, V. Aggarwal, R. Jana, K. Ramakrishnan, C. W. Rice, and N. Shankaranarayanan, "Design and characterization of a full-duplex multiantenna system for wifi networks," *IEEE Transactions on Vehicular Technology*, vol. 63, no. 3, pp. 1160–1177, 2014.

[73] C. Coates, "Flow-graph solutions of linear algebraic equations," *IRE Transactions on circuit theory*, vol. 6, no. 2, pp. 170–187, 1959.

[74] S. J. Mason, "Feedback theory-some properties of signal flow graphs," *Proceedings of the IRE*, vol. 41, no. 9, pp. 1144–1156, 1953.

[75] I. S. Gradshteyn and I. M. Ryzhik, *Table of integrals, series, and products*. Academic press, 2014.